Kwinana Air Modelling Study

INTENSIVE EPISODE STUDY WORKSHOP

Papers presented at a workshop 29th August 1978

DEPARTMENT OF
CONSERVATION & ENVIRONMENT
WESTERN AUSTRALIA

BULLETIN No 54

81662/12/78 100 R80

KWINANA AIR MODELLING STUDY

WORKSHOP ON MARCH 2, 1978 INTENSIVE EPISODE

Papers Presented

Held on August 29, 1978 at the Physics Conference Room, WAIT

CONTENTS

PREFACE

As part of the Kwinana Air Modelling Study intensive experimentation was carried out on March 2, 1978. An important part of this work involved the release of two tracers from a stack at the SEC's power station at Kwinana and the collection of air samples downwind of the release. The samples were analysed and a picture of the tracer distribution was constructed.

Meteorological information was obtained from the two base stations being used in the study, five anemometers, two acoustic sounders and a number of radiosonde releases.

All of the above data together with aerial and ground photography of plumes and emissions of sulphur dioxide from industry at Kwinana has been compiled in Environmental Note 33 "Kwinana Air Modelling Study - Tracer Experiment 1".

The following papers presented at a workshop on the March 2 intensive episode represent an attempt to draw some conclusions about the meteorology and air pollution potential of the Kwinana industrial region under summer sea-breeze conditions. Detailed and valuable discussions of the ideas put forward were held during and after the delivery of each paper.

ATTENDANCE

Dr. W. Walker Dr. M.J. Lynch Dr. N.E. Holmes Dr. G. Allan Dr. P. Rye	Physics Department, WAIT
Dr. T. Lyons Mr. F. Kamst	School of Environmental and Life Sciences, Murdoch University
Dr. J. Carras	School of Mathematical and Physical Sciences, Murdoch University
Dr. J. Patterson	Civil Engineering Department University of W.A.
Mr. A. Scott	Bureau of Meteorology
Dr. D. Martin Mr. G. Hepworth	Clean Air Section Public Health Department
Dr. B. Hamilton Mr. K. Rayner Mr. V. Paparo	Department of Conservation and Environment
Apologies: Mr. R. Powell	Clean Air Section, Public Health Department

The Meteorology at Kwinana

March 2 1978

Alan Scott

Bureau of Meteorology

1. GENERAL CONDITIONS

This day was rather typical of a number of the hot days which occur near Perth in the summer months. Near ground level a light to moderate E/NE airflow existed in the morning over the southwest of the State with a low pressure trough off the west coast and E/SE winds west of the trough (Fig.1). As would be expected the broad scale flow in the layer up to 1000 m was similar to that at the surface but at 1500 m wind directions near Perth were ESE (Figs. 2 and 3). In the early morning the radiosonde release from Perth Airport showed an inversion layer between the surface and 600 m. If this layer was uniform across the coastal plain convective mixing would have caused its dissipation by about 10.15 a.m. at Wattleup when the surface temperature reached 32°C.

Maximum temperatures recorded are shown in Table 1 below. The strong gradient of maximum temperature between the coast and locations only a few kilometres inland is very evident.

Location	Minimum °C	Maximum °C
Perth Airport	21	38
Perth	25	37
Fremantle	20	35
Wattleup		34.4
Kwinana		31.6
Garden Island	24	33
Rottnest Island	24	34
Alcoa F. Lake		38

TABLE 1: Minimum and maximum temperatures recorded in the region.

A sea breeze developed on the coast near Kwinana at about 9.30 - 10.00 a.m. This breeze gradually extended both inland and seawards as portrayed in Figures 4-8. The rate of eastward movement of the sea breeze during the three hour period after 10.00 a.m. averaged about 0.8 m/sec (3 km/h) though there appears to have been an acceleration during this period (Fig.9). The rate at which the sea breeze developed seawards seems to have been approximately

twice the early eastward movement although the confidence attached to this statement is reduced by the rather arbitrary positioning of the seaward extent of the sea breeze particularly at 10.00 a.m. Rottnest Island reported a 5 m/sec easterly wind at noon thus indicating that the sea breeze circulation was probably not close to that location.

Measurements of the horizontal wind direction variance, sigma, at the Kwinana and Wattleup base stations generally reflected the expected changes in stability (Fig. 11). At Kwinana large values of sigma occurred until the sea breeze was established at about 10.00 a.m. The increase in sigma values at this site after 3.00 p.m. is difficult to explain. Sigma values at Wattleup show the morning convective instability and the arrival of the sea breeze between 11.00 a.m. and noon followed by a more stable air mass. The high sigma values just before 2.00 p.m. and 3.00 p.m. are not evident on the Mt. Brown anemometer records but evidence that they are probably real is shown by the strong correlation between the later readings and the high sulphur dioxide levels measured at this time at Wattleup.

The concentration of sulphur dioxide at the Wattleup site is shown by the data in Fig.10 to be strongly related to wind direction (and also as mentioned to the prevailing stability). Sulphur dioxide was detected in significant quantities when the mean wind direction lay between about 215 and 235^{o}.

2. METEOROLOGICAL CONDITIONS DURING THE TRACER RELEASE AND SAMPLING PERIOD

During this period a fairly steady southwesterly sea breeze of 4-6 m/sec prevailed both near the coast and over the adjacent parts of the coastal plain. Temperatures remained fairly steady at about 31^{o} at Kwinana and 31-32^{o} at Wattleup. At Alcoa's F Lake the temperature was about 36-37^{o} during the period from 2.00 - 3.15 p.m. It is worth noting that at the Perth Regional Office of the Bureau of Meteorology the temperature fell steadily after the arrival of the sea breeze at about 12.40 p.m. to be 34.4^{o} at 3.00 p.m.

Between one quarter and three quarters of the sky were covered by thin cirriform cloud. The variations in total global radiation show the effects of this.

Low level radiosonde flights at Alcoa's F Lake indicated only a slight wind shears between the surface and 400 m during the tracer period (Fig. 12). At the same time a super adiabatic lapse rate existed in the lowest 100 m with the layer between 100-450 m having a lapse rate near the dry adiabatic (Fig.13). A weakly stable (isothermal) layer was detected between 450-550 m. This corresponded with the interface between the SW sea breeze and the over-riding ESE winds.

The mixing depth measured by the WAIT acoustic sounder at the Kwinana base station during the tracer experiment was about 300 m. The Murdoch sounder at Alcoa's F Lake indicated a mixing depth of about 400 m which is in reasonable agreement with the radiosonde data.

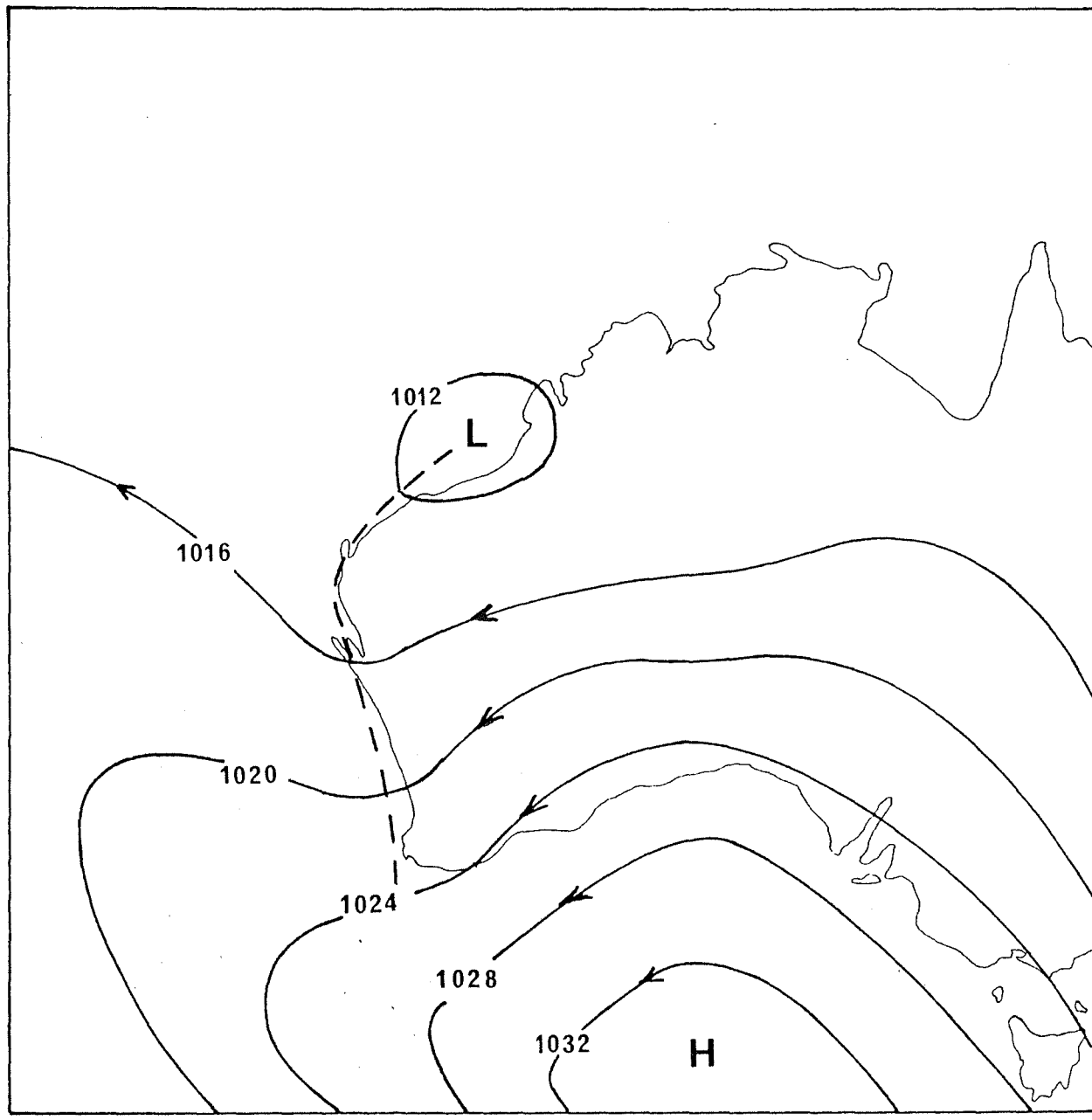

FIGURE 1 Mean sea level analysis 0900 WST 2 March 1978

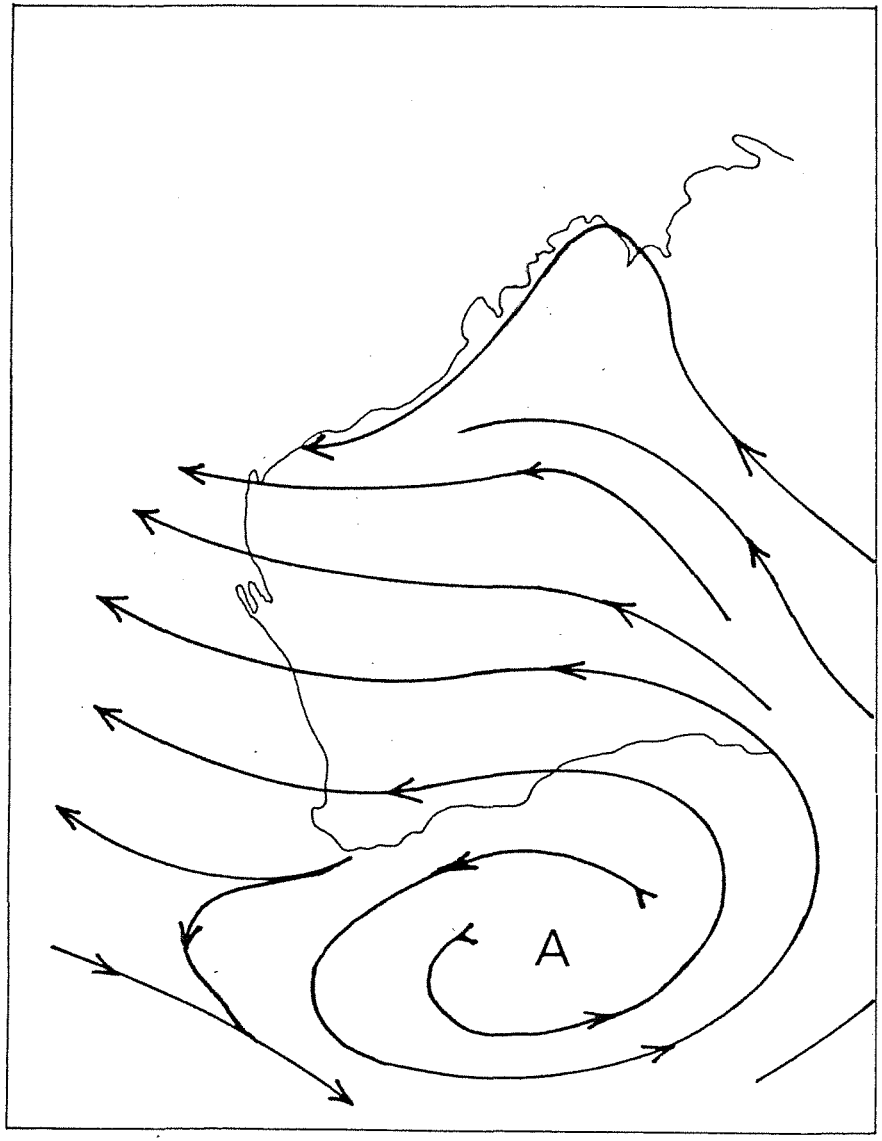

FIGURE 2 1000 m streamline analysis
1300 WST 2 March 1978

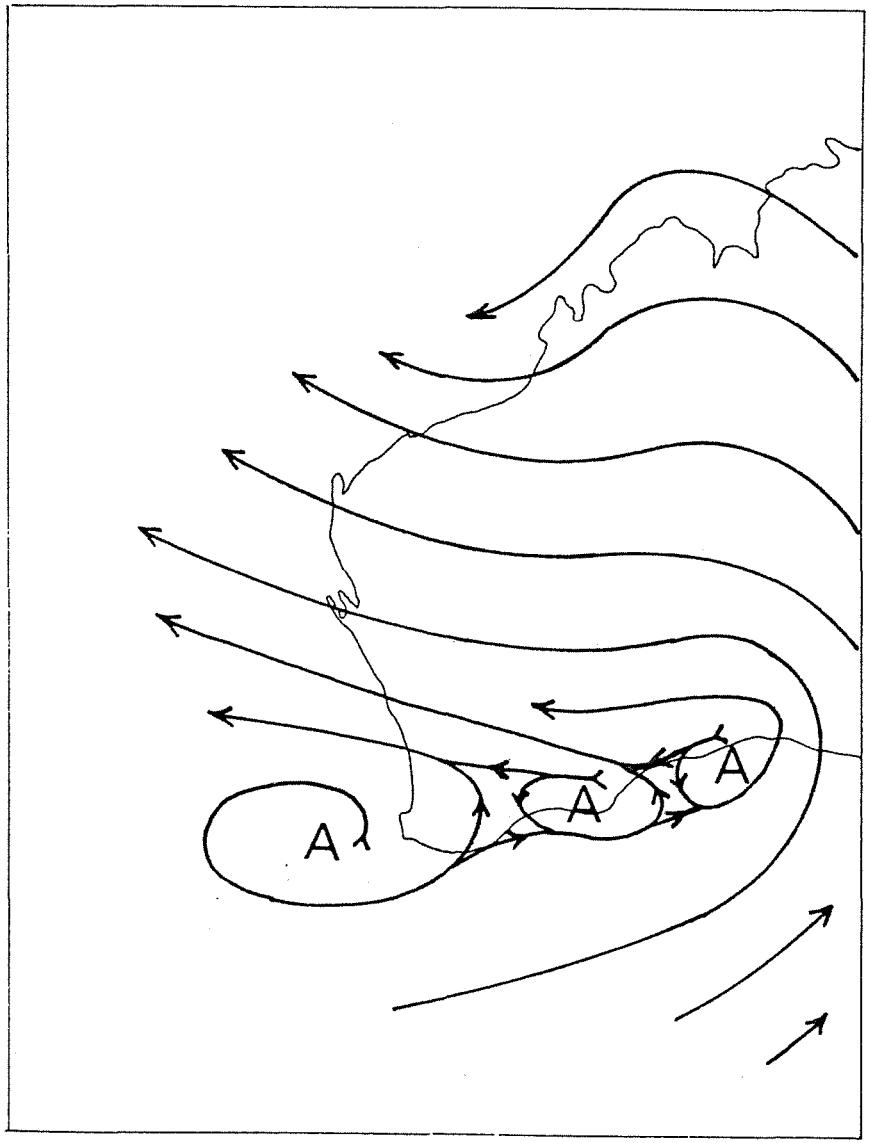

FIGURE 3 1500 m streamline analysis
1300 WST 2 March 1978

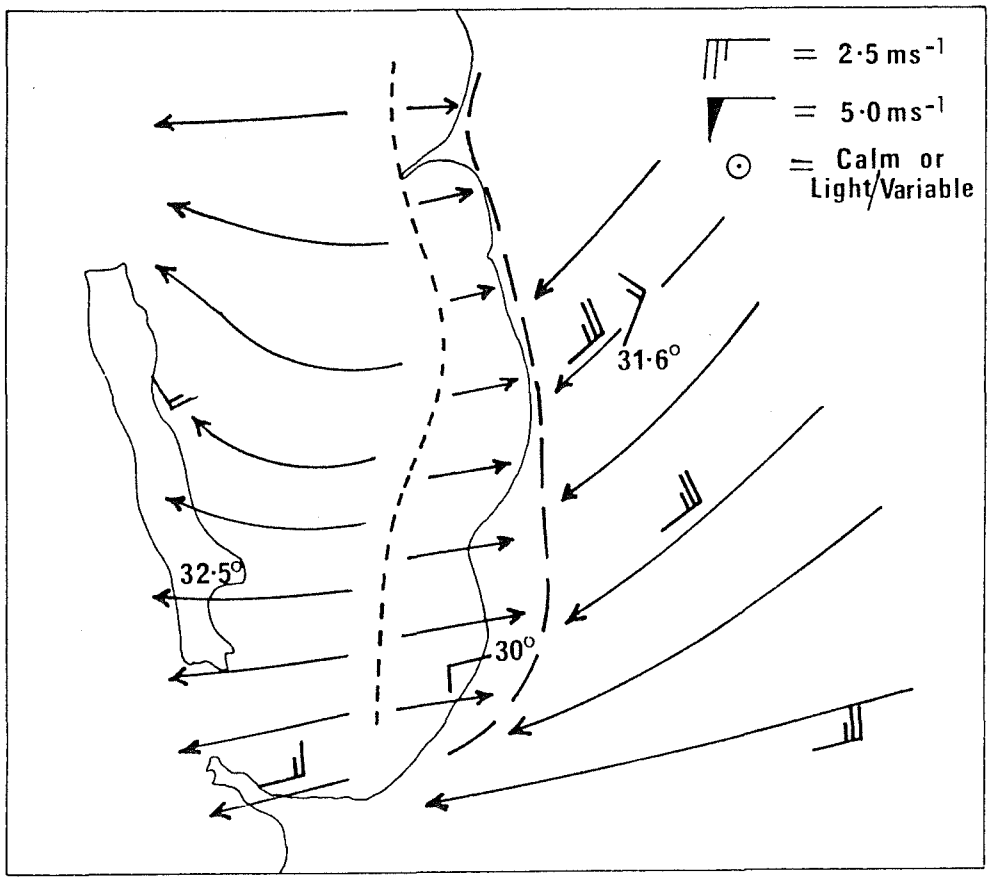

FIGURE 4 Streamline analysis for the Cockburn Sound-Kwinana area 1000 2 March 1978

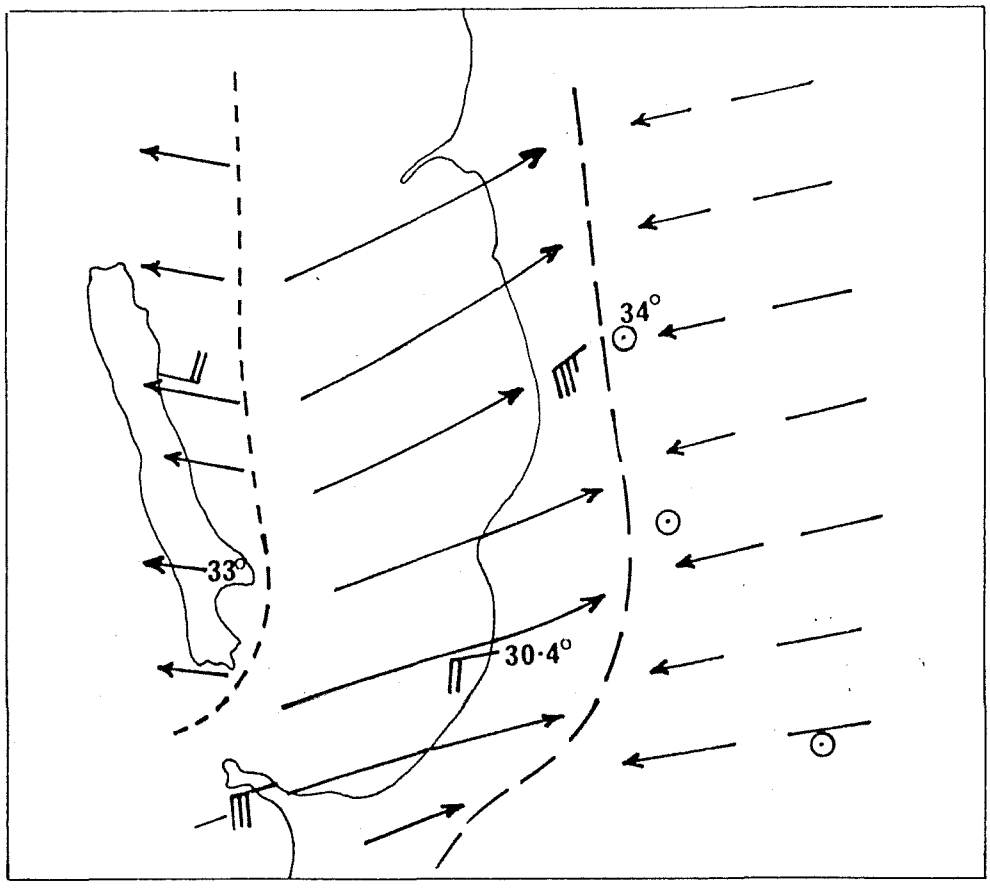

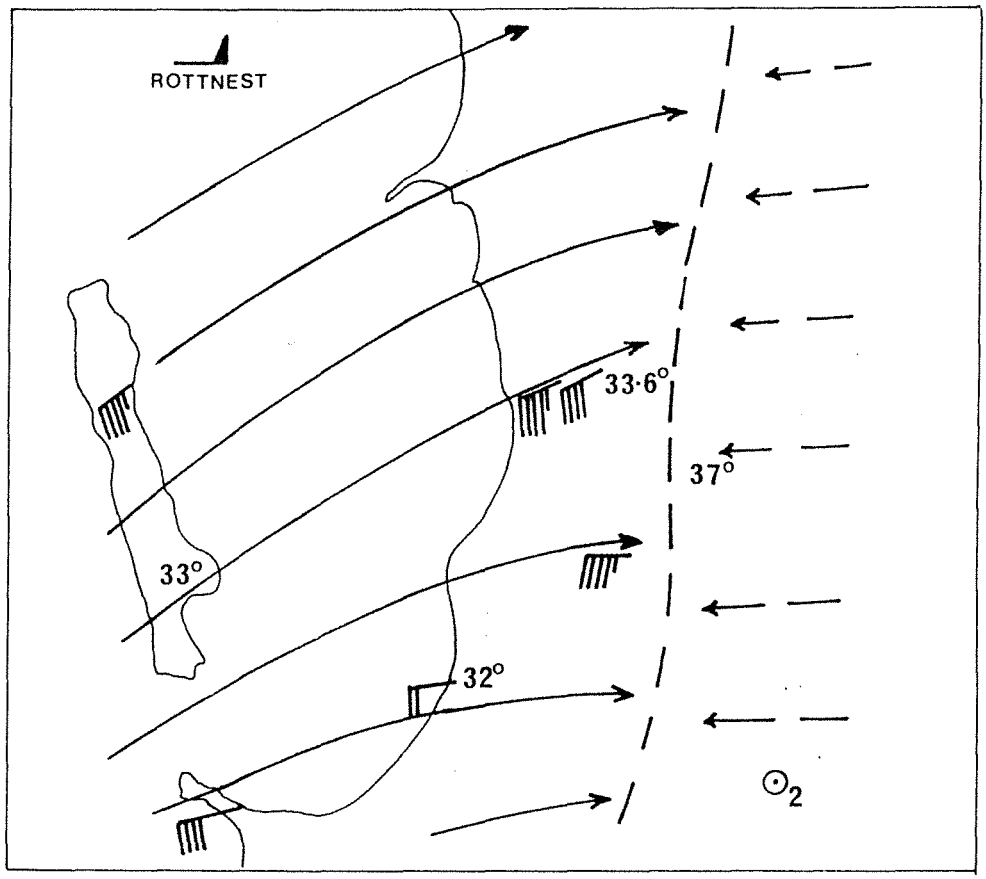

FIGURE 6 Streamline analysis 1200 2 March 1978

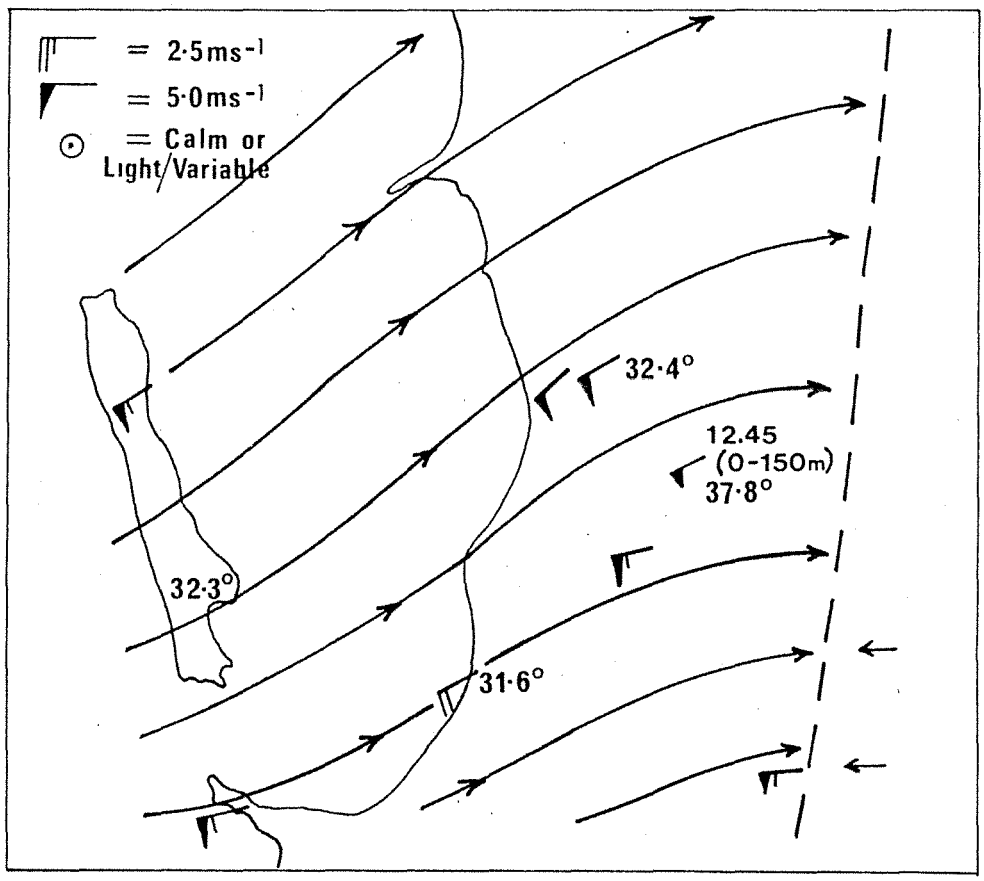

FIGURE 7 Streamline analysis 1300 2 March 1978

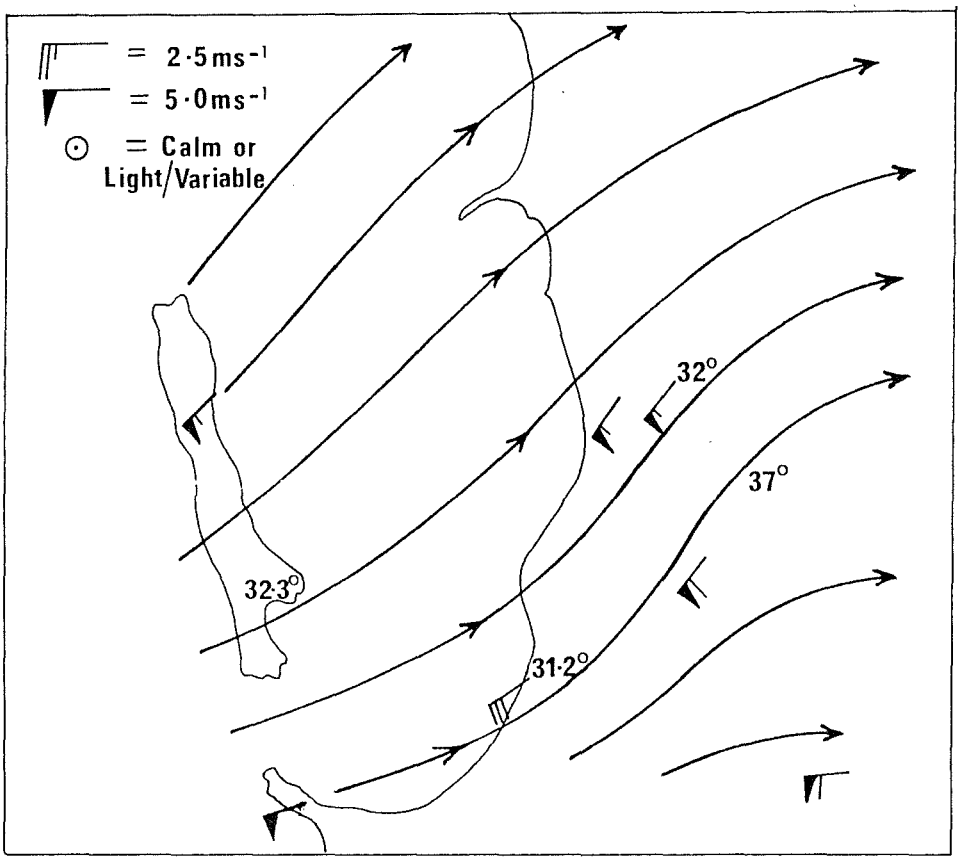

FIGURE 8 Streamline analysis 1400 2 March 1978

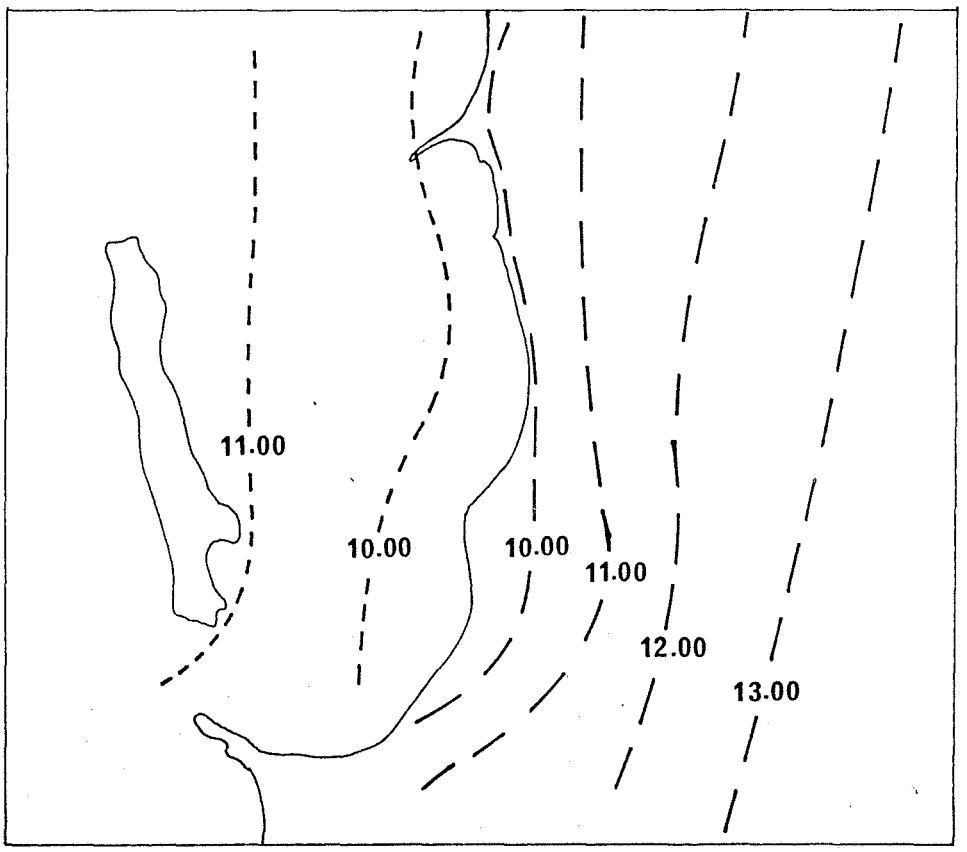

FIGURE 9 Positions of the inland and seaward extent of the sea breeze circulation at hourly intervals on 2 March 1978

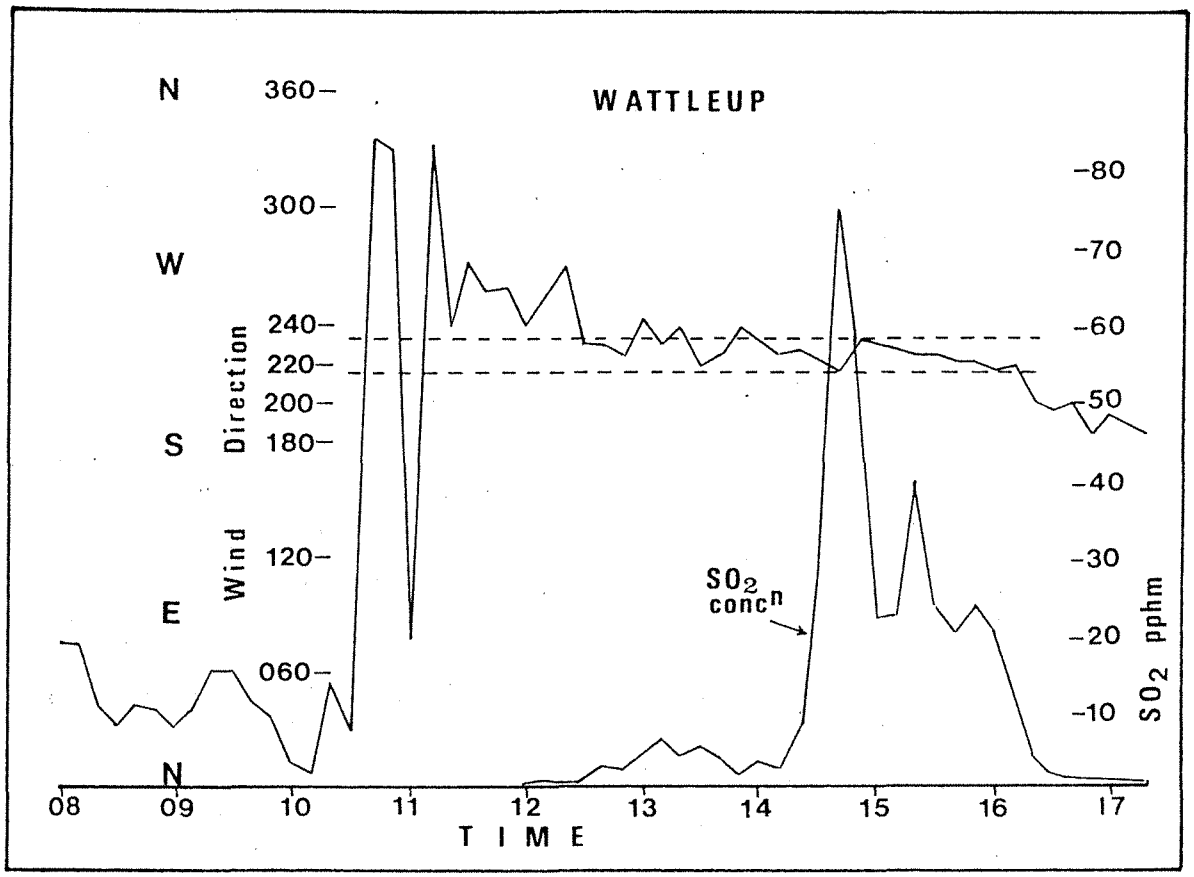

FIGURE 10 Sulphur dioxide concentrations at Wattleup related to wind direction (2 March 1978)

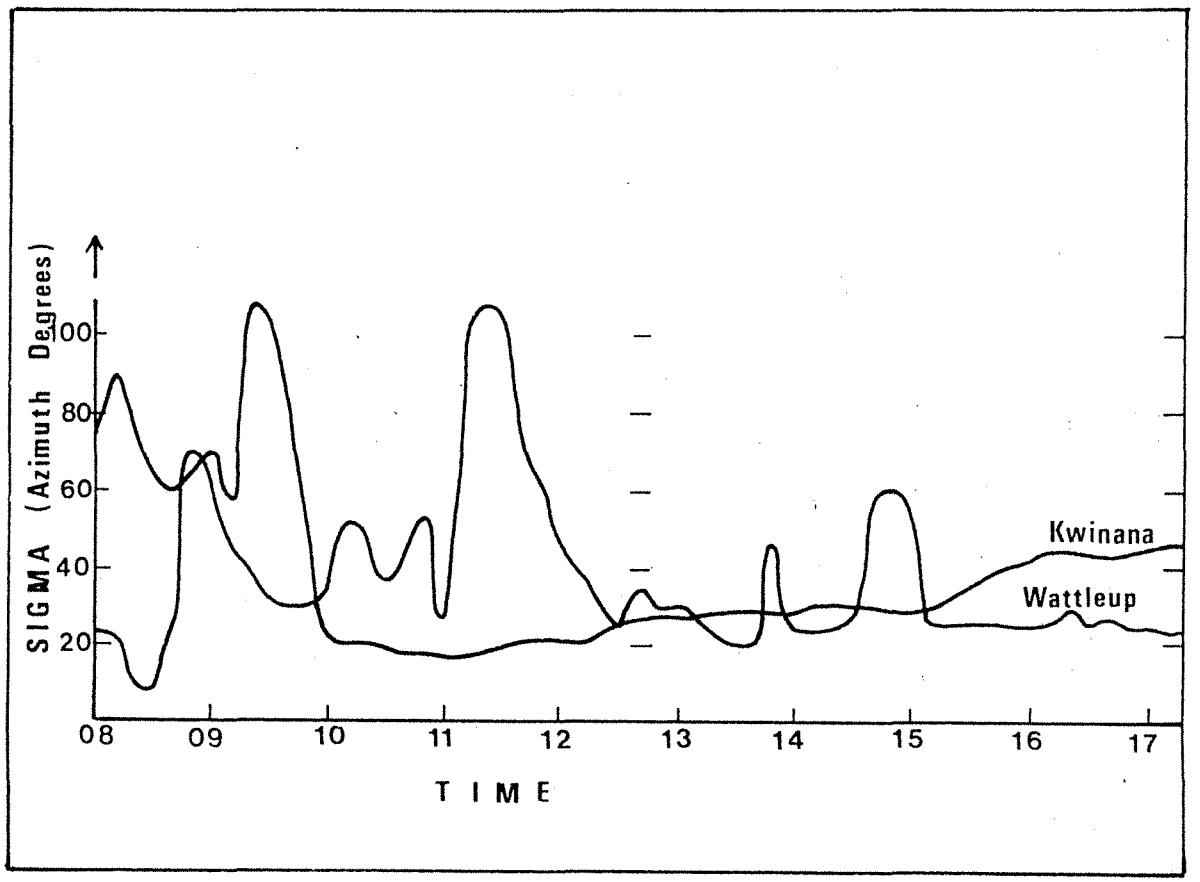

FIGURE 11 Wind direction variance, sigma, at Kwinana and Wattleup on 2 March 1978

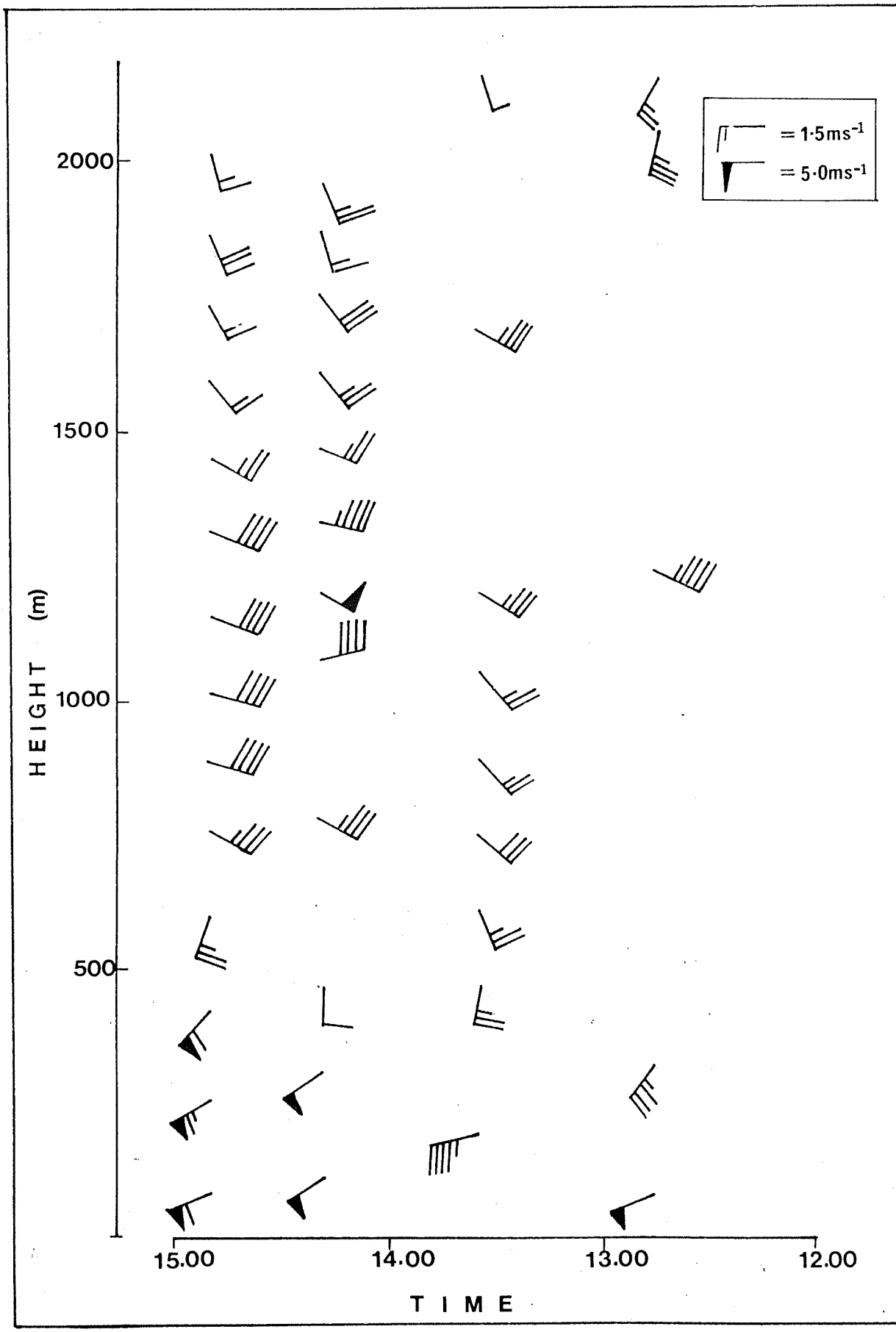

FIGURE 12 Low level winds measured at Alcoa's F Lake 2 March 1978

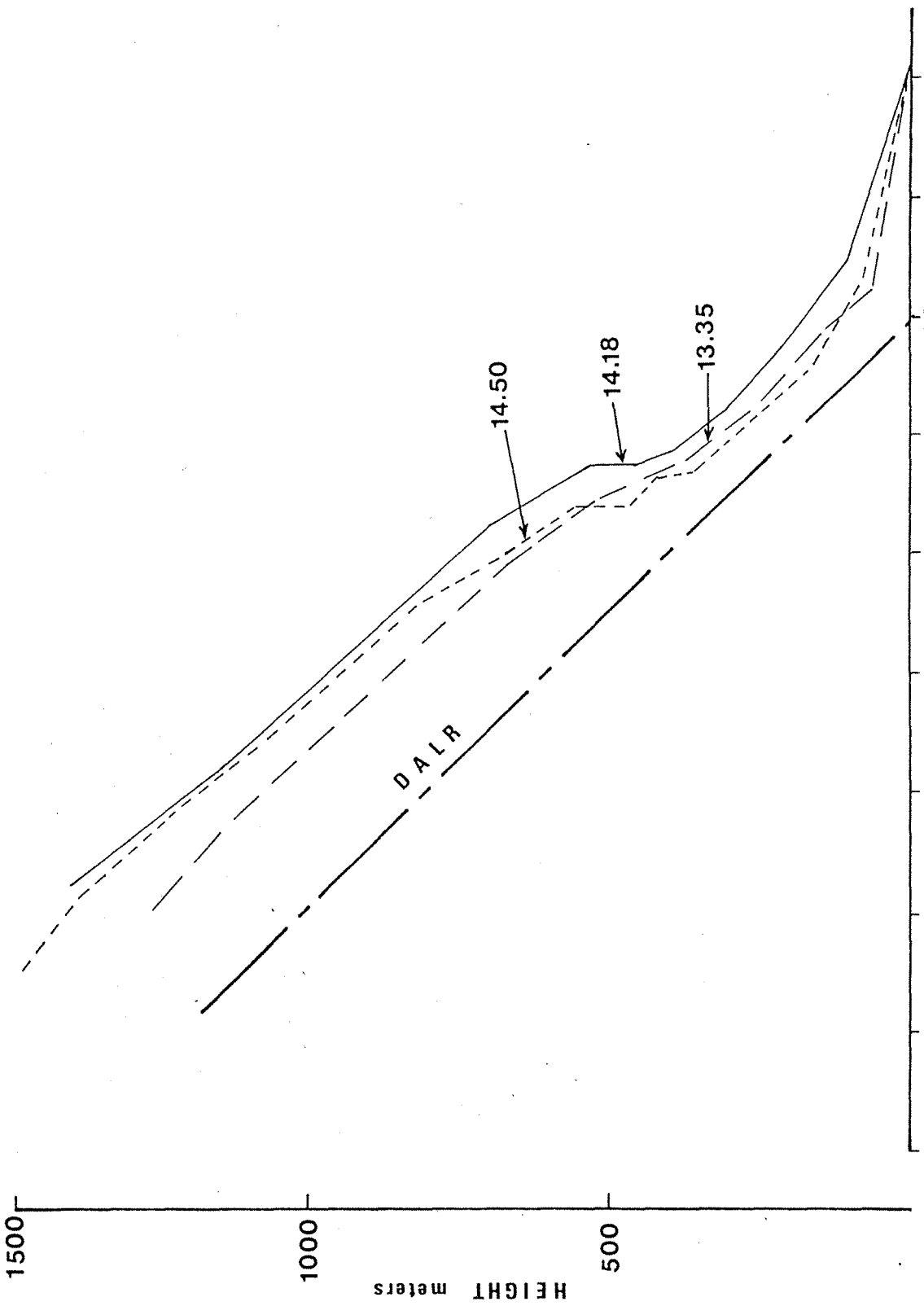

FIGURE 13 Low level temperature data measured at Alcoa's F Lake 2 March 1978

A Study of the Wind Field at Kwinana

F. Kamst

School of Environmental and Life Sciences,

Murdoch University

1. INTRODUCTION

A major industrial site is located at Kwinana, 32 km southwest of Perth, the capital of Western Australia (see Figure 1). An initial air pollution study was undertaken at Coogee, about 2 km north of Kwinana, during 1973 and early 1974 and results are reported in the Coogee Air Pollution Study (1974). A second study, the Kwinana Air Modelling Study, centered on Kwinana and covering an area of 10 km by 15 km, was commenced in 1976. Wind speed, wind direction, temperature, and relative humidity are continuously recorded and SO_2 levels sampled. This report deals with wind speed and wind direction data. Its aim is to describe the windfield in the Kwinana area and explain the effects of topography on the horizontal surface winds so that the atmospheric transport of pollutants emanating from the industrial area can be better understood.

2. CLIMATE

Perth's climate can be defined as Mediterranean (Gentilli, 1971), consisting of hot, dry summers and mild, wet winters. On the synoptic scale, winds are governed mainly by the position of the anticyclonic belt which lies east-west off the south coast of Western Australia in summer and moves northward across the state in winter (Bureau of Meteorology, 1969). In summer, easterlies prevail; however these are usually disrupted by a reliable sea breeze (the "Fremantle Doctor"), which produces a higher average windspeed than at any other time of the year. In winter, depressions originating in the Indian Ocean or Southern Ocean pass close to the south coast of Western Australia which bring rain sometimes accompanied by strong westerly winds (Bureau of Meteorology, 1969).

3. TOPOGRAPHY

Figure 1 shows the Kwinana Air Modelling Study area. It is located on a coastal strip up to 15 km wide, to the west of which is Garden Island (approximately 10 km long and 1.5 km wide), separated from the mainland by Cockburn Sound.

The northern part of Garden Island has an even topography, whereas the southern part has sandhills with heights up to 50 m. At the northern extremity of the coastal study area is Mt. Brown (70 m high). On the western side of Mt. Brown lies a narrow strip of flat land, which is adjacent to the coast and extends southward increasing to a maximum width of 9 km. To the east of this is an

area, approximately 4 km wide, of low hills (up to 50 m high), with flat country further eastward.

4. INSTRUMENTATION AND DATA REDUCTION

Five Lambrecht Woelfle anemometers were installed at the beginning of 1976 and their positions are shown in Figure 1. The choice of sites was subject to the criteria that a well-spread network be available, that local influences such as nearby trees or gullies be avoided in order to obtain data representative of the surrounding area, and that the risk of vandalism be minimized. Site 1 is situated on a pig farm surrounded by low hills about 15 m high. Site 2 is on the western slope of Mt. Brown and is approximately 40 m above sea level. Site 3 is 15 km inland from the coast, situated in flat pasture country. Site 4 is located at the southern side of Cockburn Sound on the coast, with dunes up to 25 m high to the north west. Site 5 is on the north eastern end of Garden Island, approximately 30 m from the beach; the land west of this site rises to a height of about 30 m, with a slope of 1 in 50.

The anemometers were calibrated for windspeed by the manufacturers, this was assumed correct,and no additional calibrations were carried out. They were mounted on power poles, between 7 and 10 m high. No attempt is made to adjust the windspeed data to a uniform height. Windspeeds are averaged over an hour and recorded in steps of 0.1 m/sec on the hour. Levelling of the anomometers was carried out when they were installed.

Wind directions are averaged over half an hour, and recorded in sectors of 10^{o}, centered on 0^{o}, 10^{o}, ... 350^{o}, every half hour. A check made on the alignment of the anemometers showed that the ones at sites 3 and 4 were misaligned by -18^{o} and -8^{o} respectively. Hence in the analyses 20^{o} and 10^{o} were subtracted from the wind direction data at sites 3 and 4 respectively, which resulted in the anemometers being effectively aligned within 5^{o} of each other.

This report uses data recorded for the twelve months March 1977 to February 1978. The effective data recovery from each site during this period is shown as a percentage. Also shown are the months during which less than 50% of the data were recovered. Several other minor gaps appeared as well.

Table 1 Data recovery of each observation site.

Site	1	2	3	4	5
% data recovery	91	95	67	91	80
months with less than 50% data recovery			Aug (29%) Sep (0%) Nov (25%) Feb (2%)	Apr. (17%)	Jan (13%)

5. FREQUENCY WINDROSES

Windroses are useful initial indicators, of the general nature of the airflow at each of the sites. Even though they give a description of the mean windfield at each site they do not contain temporal and spatial variation of the flow as it moves across the area. Lyons (1977) points out that for mesoscale flow the windrose should only be used as a guide to the initial identification of important localized effects and not as the sole representation of the flow.

Windroses were plotted for each month for each observation site from the hourly data. Nine sectors of 45^{o} were used, centered on 0^{o}, 40^{o}, 80^{o}, 120^{o}, 160^{o}, 200^{o}, 240^{o}, 280^{o} and 320^{o}. The windspeeds were divided into intervals of 1 m/sec, centered on 1, 2, 3 m/sec. Calms, variable winds (those cases where a mean windspeed but no meaningful direction could be specified) and out or order readings are also included in the figures. Windroses for four months, March, July, October and December, representing each of the four seasons, are shown in Figures 2-5.

Figure 5 shows that in summer the majority of winds have a south westerly or easterly component, which represents the sea breeze and the synoptic (anticyclonic) influences repectively (see Section 2). Near the coast the sea breeze is strong, up to 12 m/sec (Figure 5(b) and (d)), while further inland both the frequency and strength of the sea breeze decrease (Figure 5(a) and (c)). It is worth noting the high frequency of variable winds at site 3 (112), which indicates that the change in regimes inland is perhaps not as well defined as it is at the coastal sites.

In autumn, see Figure 2, the sea breeze is still evident, but during the night the winds tend to be north easterlies to easterlies, compared with easterlies and south easterlies during the summer. There is also an increase in calm conditions inland (Figure 2 (a) and (c)), which may be due to the stabilizing influence of a cooler air mass. This is a well known process whereby, as the surface temperature falls, a strong inversion develops at lower levels and prevents the mixing of surface air with the air at high levels (Borgelt,Lyons and Scott, 1977). This results in lower average wind speeds at the surface (Bureau of Meteorology, 1969).

Figure 3 shows that in winter high north easterlies are predominant while winds from the north west, which bring the rains, are less frequent but stronger. At sites 2 and 4 north easterly winds are stronger than easterly winds;both occur with a similar frequency. The north easterlies at sites 1 and 3 are more frequent than easterlies. Hence it appears that when calms are recorded inland, winds near the coast are predominantly easterlies.

In spring there is a return to the summer conditions with a sea breeze evident, although not well developed (Figure 4).

6. HODOGRAPHS

The temporal and spatial variations of air flow across the study area can be studied in a qualitative way by means of monthly hodographs. A hodograph represents the locus of the end points of the resultants wind vector for each hour of the day. Hence the resultant vector.

$$\overline{V} = \underline{i}\,\overline{u} + \underline{j}\,\overline{v} \qquad \text{(i)}$$

can be calculated, where $\underline{i}$ and $\underline{j}$ are unit vectors and $\overline{u}$ and $\overline{v}$ the averages of all the west and south components of the winds for the month at a given hour.

The hodographs for summer, shown in Figure 6, are elliptical in shape. Lyons, (1975a), in a similar analysis, following Staley (1957), has shown that hodographs of this kind are representative of a sea breeze/land breeze circulation. The sense of rotation at each site is anti-clockwise, except when the sea breeze establishes itself. This is in agreement with the coriolis deflection of the flow.

If we define the onset of the sea breeze when the wind first assumes a westerly component, then the sea breeze first appears at the coast south of Garden Island. Twenty minutes later the sea breeze circulation extends to site 2, while after a further twenty minutes the sea breeze becomes apparent at sites 3 and 5. Finally the sea breeze becomes established at site 1 twenty minutes later. This development of the sea breeze is shown in Figure 8.

The onset of the sea breeze is characterised by a southerly wind near the coast, however, inland there is no preference (Figure 6). It appears from Figure 6, that the large number of variable winds recorded at site 3 and to a lesser extent at site 1 (see Figure 5(a) and (c)) occur during this period. These observations have importance for air pollution studies in the region. It is possible that pollution exhausted into the atmosphere before the sea breeze has developed will be transported over Cockburn Sound by easterlies and returned when the seabreeze is established. Lyons (1975 b) observed this phenomenon in a lake breeze at Lake Michigan. This could lead to high levels of pollution in coastal regions, particularly when the sea breeze is weak.

At night the easterlies are re-established rather abruptly at site 3, while near the coast this return is more gradual and occurs about two hours later (Figure 6).

The maximum windspeeds during the sea breeze are between 2 and 4 pm and a little later at site 4, where the speeds are highest (average of 7 m/sec). Between 11 am and 4 pm the sea breeze is generally constant in direction at each site while increasing in strength.

The hodographs in Figure 6 also show a noticeable turning of the seabreeze, there is an anti-clockwise turning of the wind across Cockburn Sound (c.f. 5 and 2, 4 and 2) and an even more pronounced turning when it moves inland (c.f. 2, 1 and 3). This turning of the sea breeze is shown in Figure 13. The turning may be a function of the roughness length, which is lower for Cockburn Sound than for the open sea, Garden Island and the mainland (see e.g. Cole (1970, pp.189-190).

Figure 7 shows the hodographs for July. It can be observed that the average windspeeds are low, and tend to be from a northerly direction. The low average speeds indicate that the winds at any given hour do not have a preferred direction as occurs during the summer. This is in agreement with the facts that winds in winter are synoptically controlled with the majority of winds being north westerlies and north easterlies (Bureau of Meteorology, 1969).

7. QUANTITATIVE SPATIAL ANALYSIS

In the previous section the temporal and spatial variations of the mesocale flow were treated qualitatively; however it is necessary to express the spatial variations quantitatively. Cehak and Pichler (1968) expressed this by means of contingency tables on a monthly basis. They used eight, 45^{o} sectors and compared the wind direction at a base site with that at another site for simultaneous observations. If the wind direction at the base site was in section i they found the percentage of cases in which the directions were concurrent (wind direction at other site also is in section i) and expressed the turning of the wind by subtracting the percentage of cases (i-1 or i-2) from the percentage of cases (i + 1 or i + 2), a positive percentage indicating a clockwise turning and a negative percentage indicating anticlockwise turning.

Although the method may work well for large mesoscale areas, the method appears unsatisfactory for the area considered here. Since the data were recorded in sectors of 10^{o}, the method of Cehak and Pichler would have to be applied using nine sectors of 40^{o}. A turning of 40^{o} across the area does not normally occur, except when the sites are under different regimes. Thus if one sector were centered on 0^{o}, another sector would encompass 225^{o}- 265^{o} which is the direction from which the sea breeze comes. Any variation within this sector is therefore not observed. This could be avoided by using smaller sectors.

Another shortcoming of this method is that percentages are calculated for any wind, which carried the implicit assumption that no matter from which direction the wind comes, it has the same characteristics. It is preferable to treat each 10^{o} sector separately. However this cannot be done on a monthly or seasonal basis, because the number of occurrences of the wind coming from some sectors may be so small as to preclude any meaningful results (see Figures 2-5).

Hence it appears that to carry out an effective quantitative spatial analysis, a whole year's data is required. This is not as unreasonable as it may at first appear. South westerly winds are mainly sea breezes (see Figures 2-5), while south easterlies to north easterlies occur mainly during the night and in particular north easterlies occur mainly during winter (See Figures 2-5).

The following method is used to eliminate the above shortcomings. Indicating the wind direction at a base site by sector i, where 10^{o} sectors are assumed, and the wind direction at another site by sector j, we define

$$Si = \frac{h_{ii}}{n_i}$$

$$Ci = \sum_{j=ih}^{i+18} hij/ni$$

$$Ai = \sum_{j=i-1}^{i-18} hij/ni$$

Where ni = total number of occurrances in sector i at the base site
nij = number of observations according to one of the above criteria
Si = percentage of concurrent directions
Ci = percentage of clockwise turning
Ai = percentage of anbiclockwise turning

A weighting scheme could be adopted, however, because of the small area considered,deviations of more than 40^{o} occur only when the area is subject to different regimes, such as the onset of the sea breeze.

If we let

$k = 0$ for $/Ci - Ai/ \leq 10\%$

$k = 1$ for $(Ci - Ai) > 10\%$ and $Ci < 50\%$

$k = -1$ for $(Ai - Ci) > 10\%$ and $Ai < 50\%$

$k = 2$ for $(Ci - Ai) > 10\%$ and $Ci > 50\%$

$k = -2$ for $(Ai - Ci) > 10\%$ and $Ai > 50\%$

graphs of k versus direction can be drawn, where $k = 0$ indicates no preferred turning, $k = 1$ and $k = -1$ indicate moderately preferred clockwise and anticlockwise turning respectively and $k = 2$ and $k = -2$ indicate strongly preferred

clockwise and anticlockwise turning. Graphs of k versus direction are shown in Figure 9 with sites 1 and 4 as base sites. Calms and variable winds are not used in the analysis, because no direction can be associated with them.

The graphs show similar features for southerly to westerly winds as for the December Hodographs (Figure 6), i.e. an anticlockwise turning across Cockburn Sound, (b) and a clockwise turning across the mainland (a) and (c). Streamlines are drawn in Figure 13. The same conclusion is reached when site 5 is used as base site.

Figure 9 (d) shows that for winds between 160^{o} and 210^{o} (southerly) the turning between sites 4 and 5 is clockwise, see Figure 10, while for wind between 310^{o}-10^{o} (north westerly to northerly) there is an anticlockwise turning. This means that as viewed from site 5 these winds turn clockwise, see Figure 11. Both these deviations can be attributed to the increased friction at Garden Island. Figure 9 (h) shows that northerly to north westerly winds tend to turn anticlockwise across Cockburn Sound, in agreement with the decrease in roughness length. The streamline for this case are drawn in Figure 12. Figures 9 (g) and (h) indicate a clockwise turning across Cockburn Sound, for easterlies and south easterlies. However this may not be a real turning. As is evident from Figure 6, the coastal and inland sites are under different regimes at the onset of the sea breeze and when the easterlies return during the mid-evening. This would appear as clockwise turning.

8. CONCLUSION

Topography does not greatly affect the windfield in most of the Kwinana area. Small scale variations, however, can occur (e.g. winds in a gully). During the summer the sea breeze commences at the south of Garden Island near the coast and then develops near the mainland in Cockburn Sound. Later the sea breeze encompasses the whole of Cockburn Sound and just inland, while to the south the sea breeze is further inland.

There is an anticlockwise turning of the sea breeze across Cockburn Sound, while it deviates in a clockwise direction (i.e. becomes more westerly) when it moves inland. The potential for high air pollution in the area occurs at the commencement of the sea breeze when pollution carried westward across Cockburn Sound is returned especially inland where variable conditions occur.
Northerly and southerly winds are deflected clockwise by Garden Island. North easterly winds tend to deviate in an anticlockwise fashion across the Sound. The majority of calm conditions inland during the winter months occur when near the coast winds are easterly. The calm or light conditions are associated with little mixing thus the potential for high air pollution in the area exists.

REFERENCES

Borgelt, M.A., T.J. Lyons and A.N. Scott
A preliminary inversion climatology for Perth, Western Australia.
Presented to Royal Meteorological Society Conference on Urban Meteorology, MacQuarie University, February, 1977.

Bureau of Meteorology (1969)
The Climate of Perth, Western Australia.
Capital City Series, C.B.M., Melbourne, 7pp

Cehak, K and Pichler, J. (1968).
Beschneibung des Stromfoldes in Alpenroich Meltels Wind Matrizon
Arch. Meb. Geogp. Biobl. Ser. A, 17 61-77

Cole, F.W. (1970)
Introduction to Meteorology
John Wiley and Sons, Inc. 300 pp

Coogee Air Pollution Study Working Group (1974)
A report for the Western Australian Environmental Protection Council, D.C.E., 140 pp.

Gentilli, J. (1971) (Editor)
Climates of Australia and New Zealand
World Survey of Climatology Vol.13
Elsevier, Amsterdam, 354 pp.

Lyons, T.J. (1975 a)
Mesoscale Wind spectra,
Quart. J.R. Met. Soc. 101, 901-910.

Lyons, T.J. (1977).
Mesoscale flow analysis
Arch. Met. Geoph. Biobl. Ser. B. 25, 233-249

Lyons, W.A., (1975b)
Turbulent diffusion and pollutants transport in shore line environments.
Lectures on air pollution and environmental impact Analysis
136-208.

Staley, D.O. (1957).
The low level sea breeze of northwest Washington
J. Meteorology, 14, 450-470.

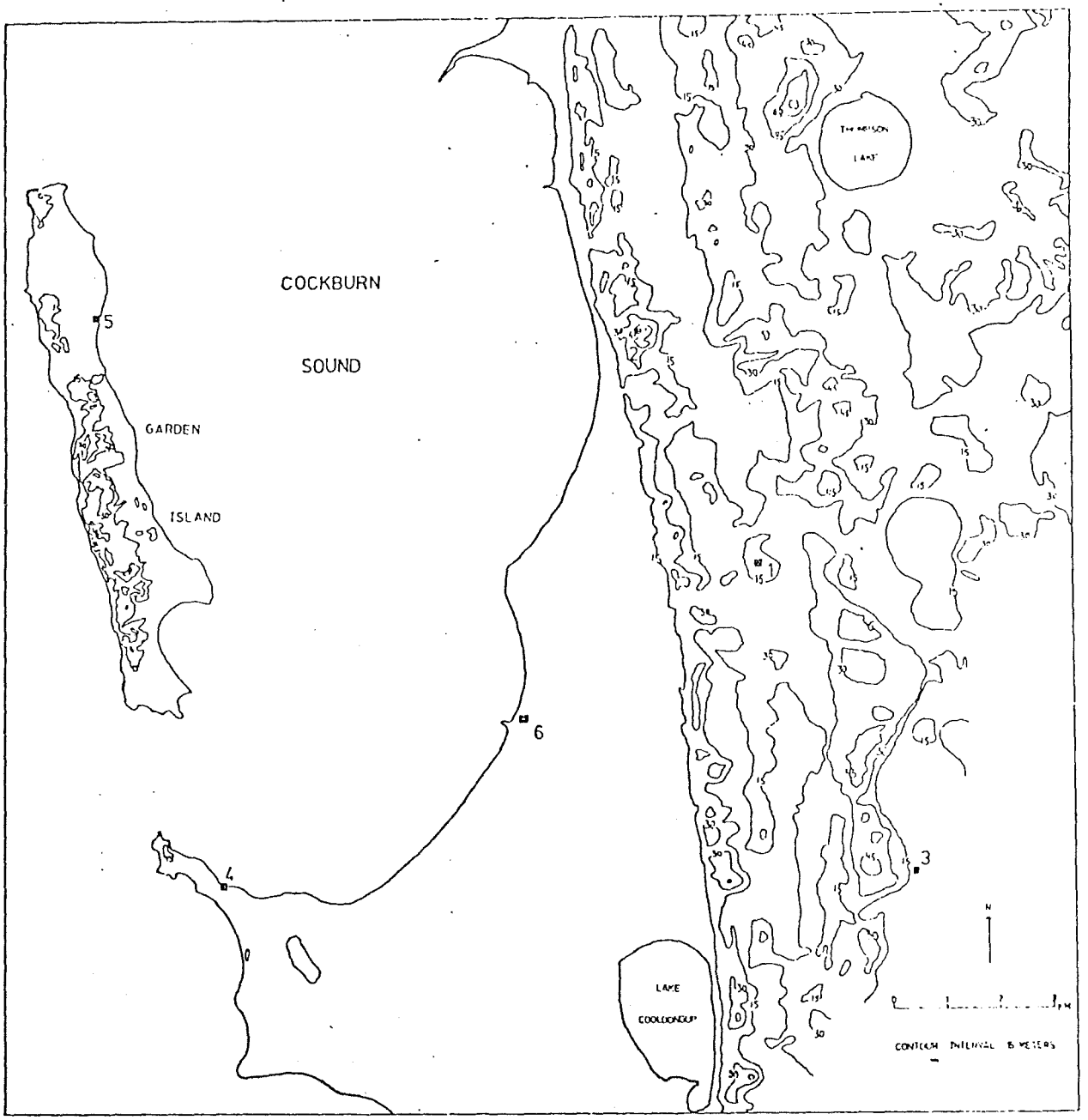

Figure.1.

Kwinana Air Modeling Study Area

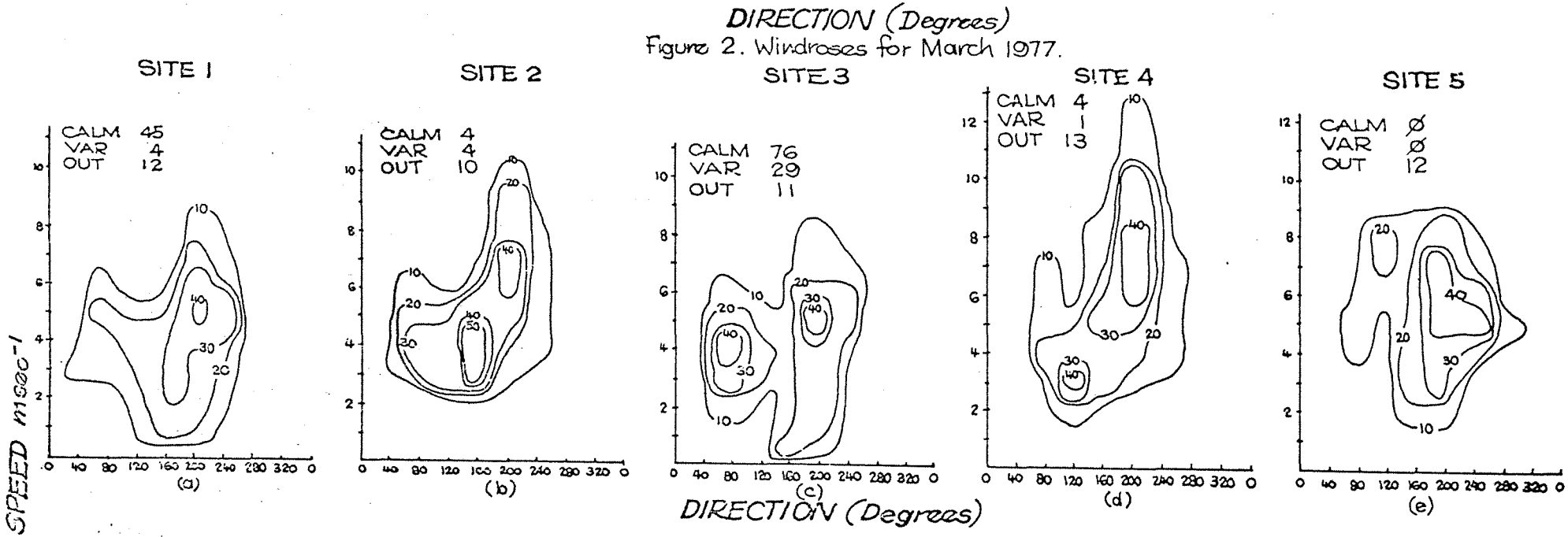

Figure 2. Windroses for March 1977.

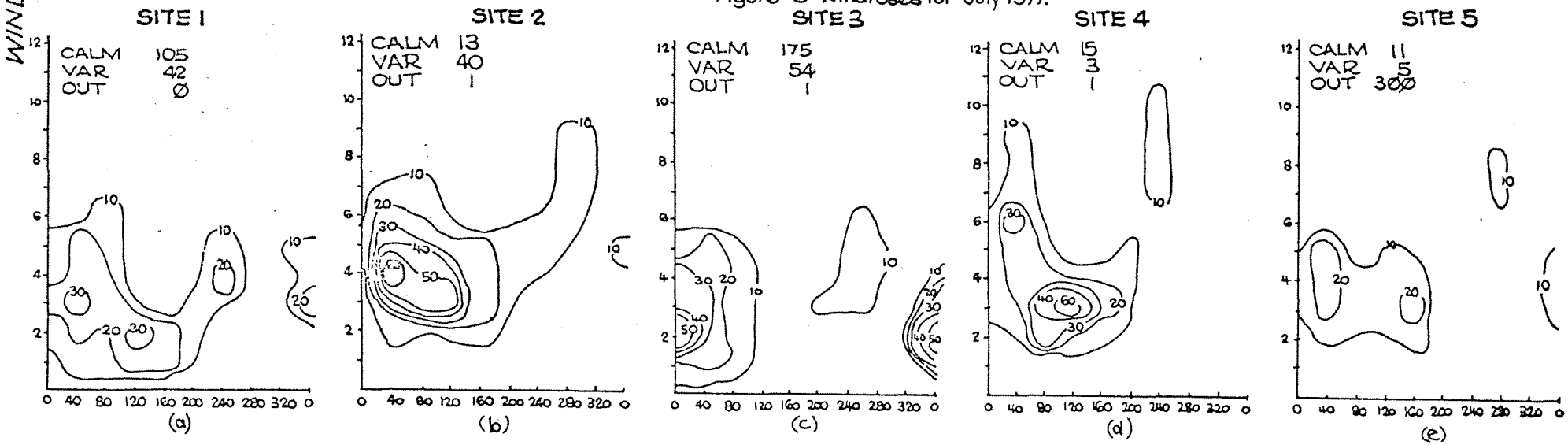

Figure 3 Windroses for July 1977.

Figure 4 Windroses for October 1977

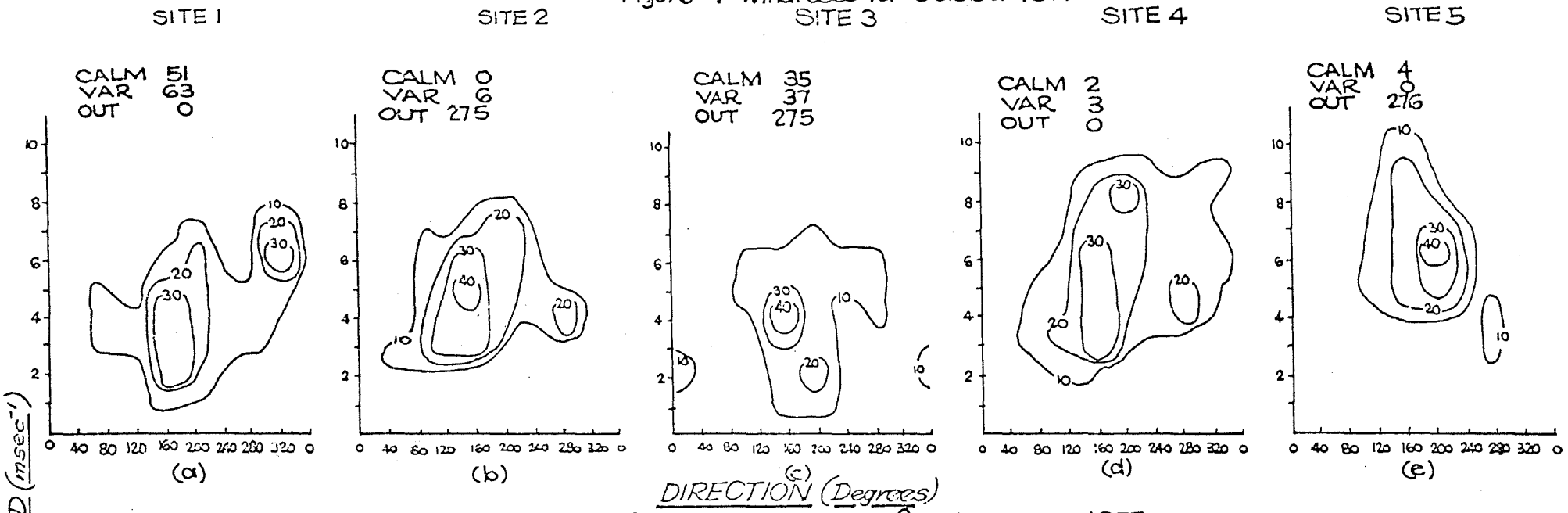

Figure 5. Windroses for December 1977

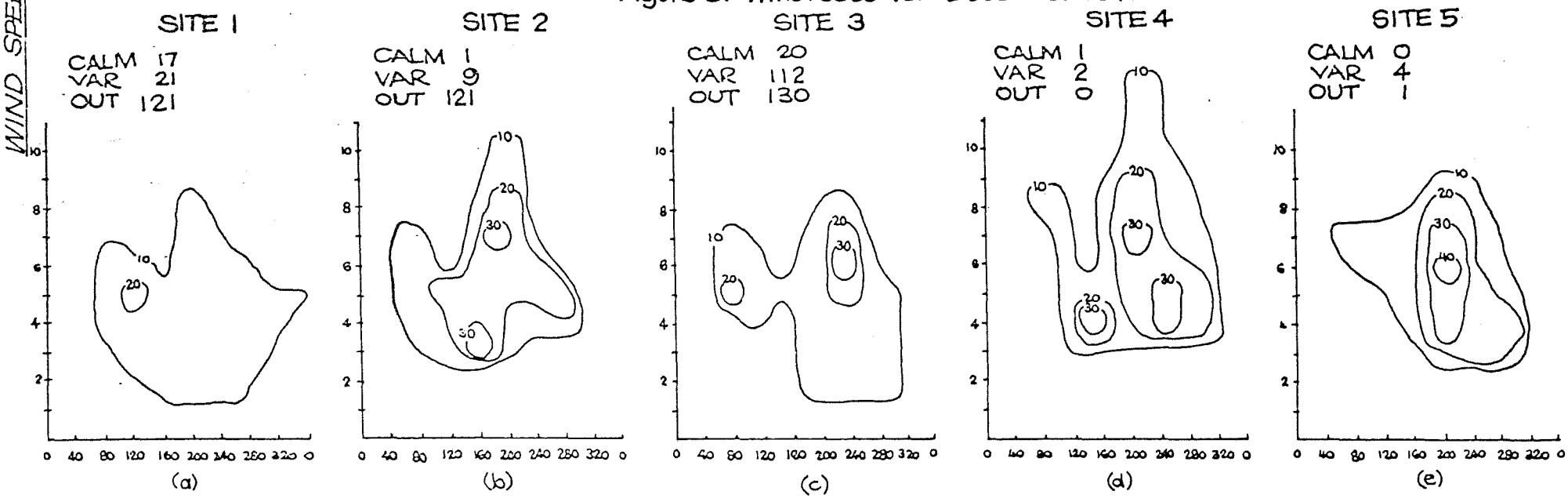

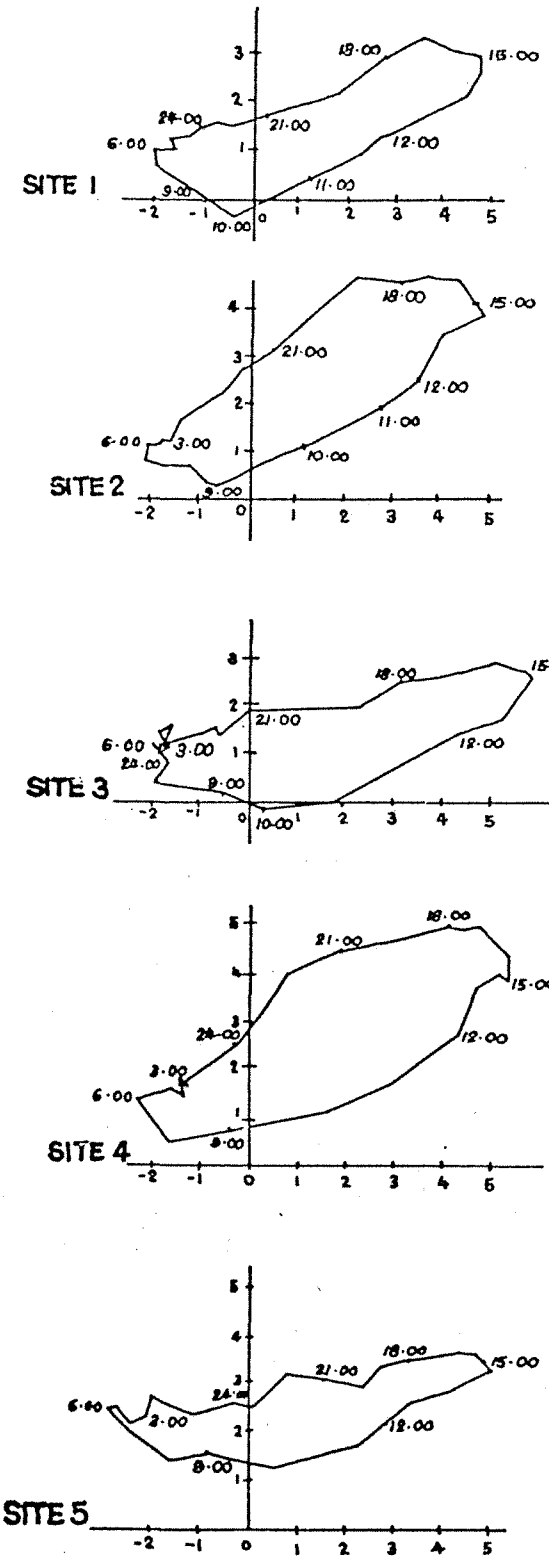

Figure 6. Hodographs for Dec 77.

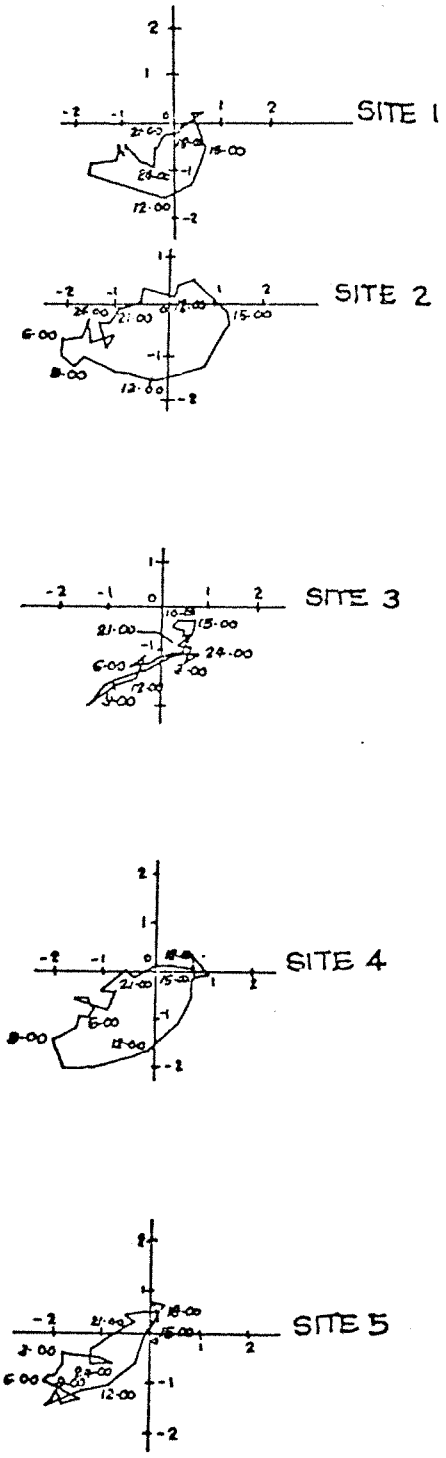

Figure 7 Hodographs for July 77.

Windspeed shown in m sec^{-1}
Times are shown on Hodographs.

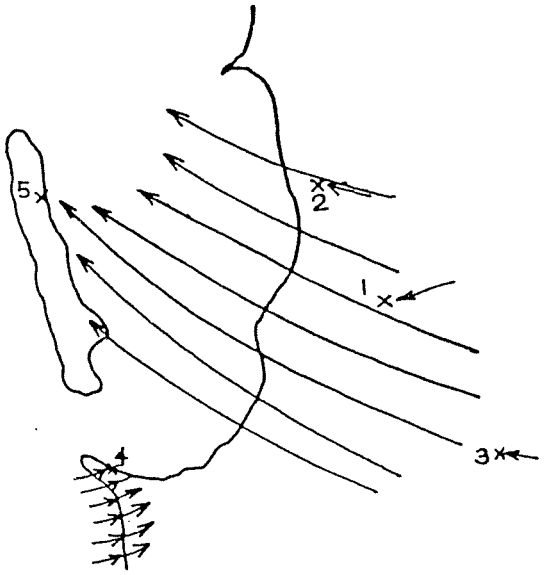

Time. 09.05

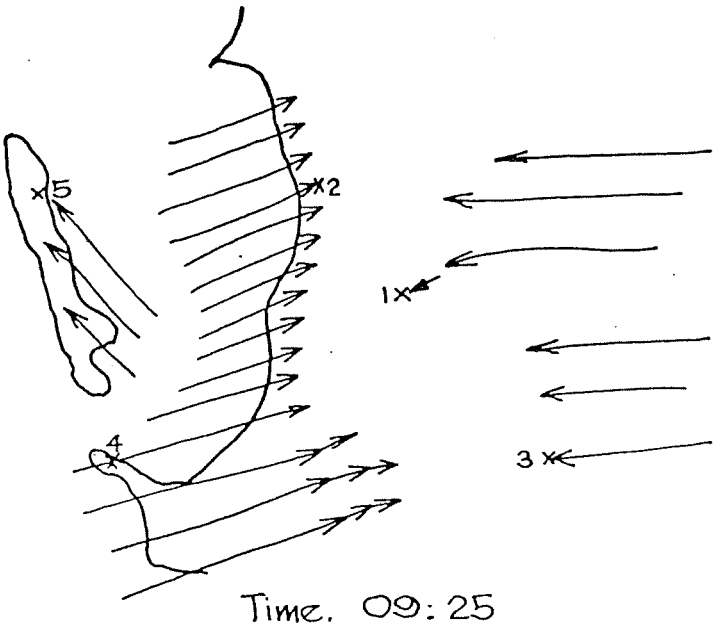

Time. 09:25

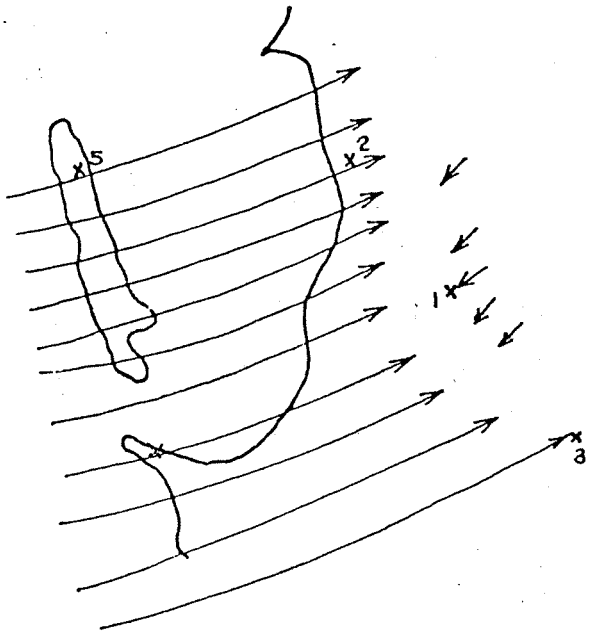

Time. 09.35

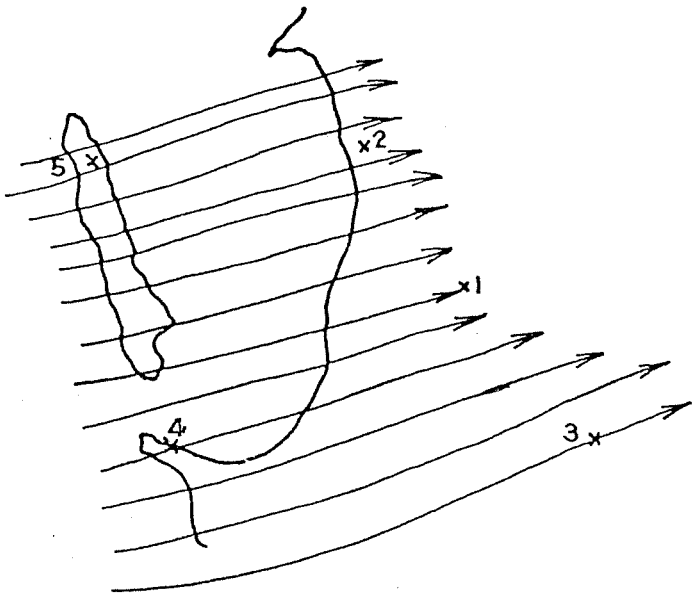

Time. 10.10

Figure 8

Development of the Seabreeze during December 1977.

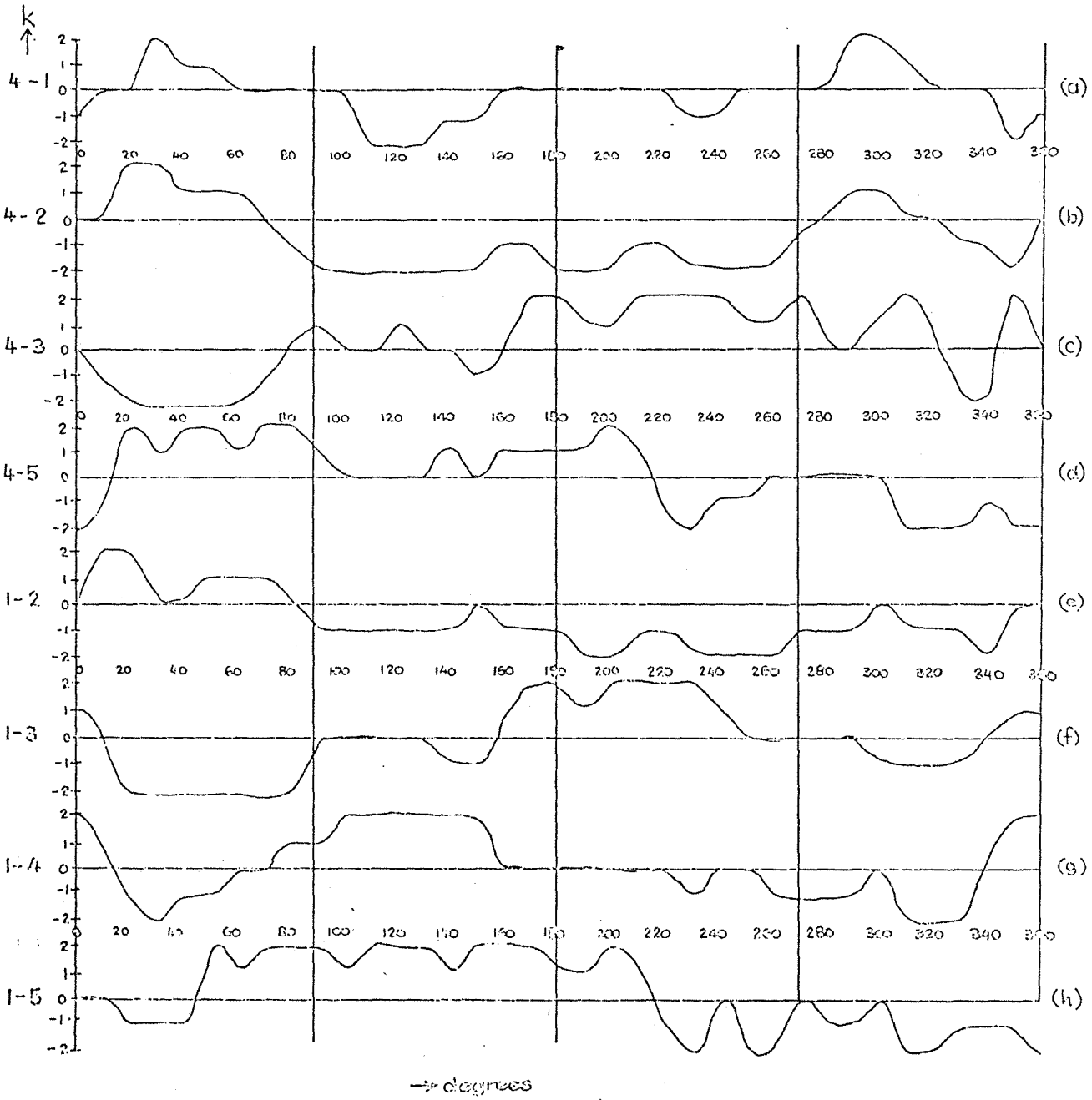

Figure 9 Graphs of k versus direction

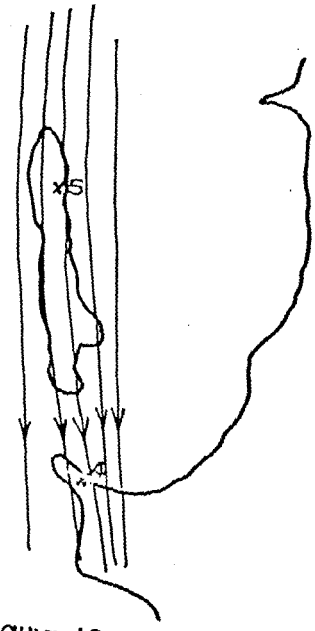

Figure 10
Streamlines for Northerly winds.

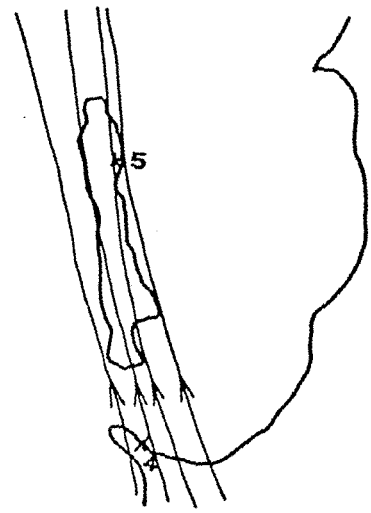

Figure 11 Streamlines for Southerly winds.

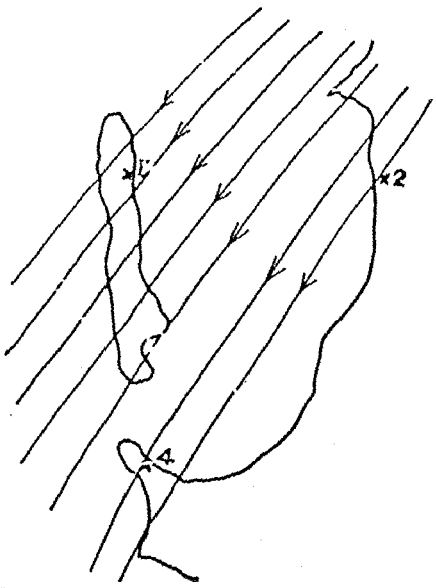

Figure 12
Streamlines for Easterly winds.

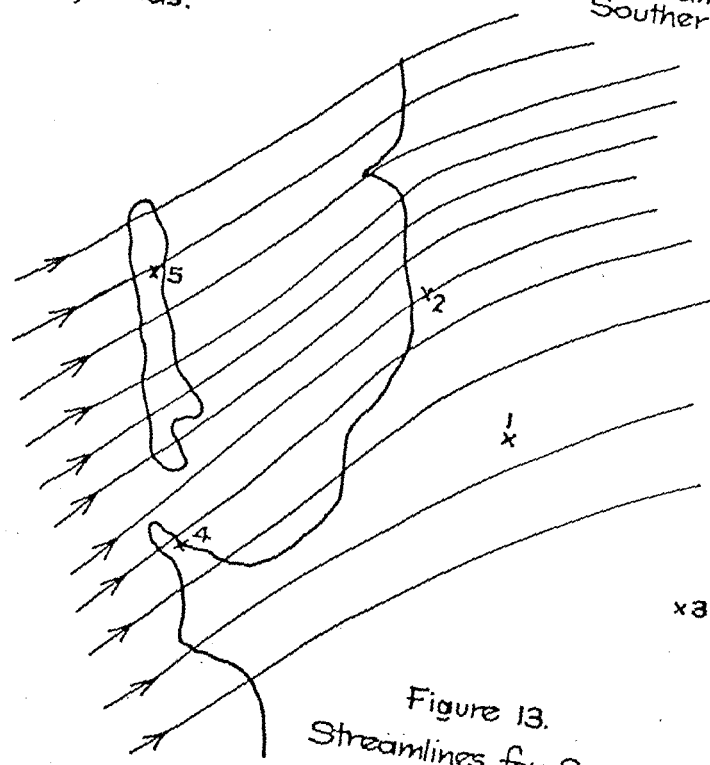

Figure 13.
Streamlines for Seabreeze.

The Anomolous March 2nd Sea Breeze: A Case of Critical Layer Absorption?

P.J. Rye

Physics Department, WAIT

1. INTRODUCTION

The W.A.I.T. Physics Department atmospheric numerical model (Rye, 1978) has been run, in its two-dimensional form to simulate the conditions which produced the "non-cooling" sea breeze observed during the KAMS field-day. Results indicate that the internal gravity waves produced in the flow above the sea breeze cell were absorbed in a critical layer at about 2 km altitude. This intensified both the horizontal and vertical motions at the top of the cell, and is proposed as the basic cause of the observed character of the sea breeze.

2. THE MODEL

The study was carried out using the numerical model described by Rye (1978 a). Apart from the elimination of a few programming errors, alterations have been made to the surface heating model (to allow for variable solar declination and to increase the stability of the surface temperature calculation) and to the calculation of "inversion height" (to improve the accuracy of the parameterisation). These improvements are described in detail elsewhere (Rye, 1978 b).

The day of year was set as the 61st (March 2nd), and the initial wind field was chosen to correspond to the 0700 W.S.T. Guildford sounding. Initial surface temperature (sea and land) was 23^{o}C. The model was run using ten horizontal grid points at 10 km spacing, and seven vertical levels on a sigma-interval of 0.04. Computation commenced at sunrise, 0540 W.S.T.

3. RESULTS

Fig. 1 shows four stages in the growth of the model sea breeze. The breeze was first resolved at 1100 W.S.T., and it is shown at this time and at hourly intervals following.

In reality, the sea breeze developed at the coast at about 0930 (Scott, private communication - see also Fig. 2). The difference is ascribed to the lack of horizontal and vertical resolution of the model, so that a narrow and shallow circulation would not be resolved. However, Fig. 2 shows a width of 9.5 km at 1100, which is in adequate, if qualitative agreement with the commencement of the model sea breeze.

Associated with the anticlockwise sea breeze cell are a pair of weak clockwise "rotors" positioned above and fractionally to the right, at the level of zero offshore wind. This location parallels the behaviour of lee waves over an obstruction in both the apparent slope of the phaselines (corresponding to one "trough" from the sea breeze front to the right hand rotor, and one from the sea breeze tail to the left hand rotor). The development of significant vertical motions is undoubtedly due to the accumulation of gravity wave energy at the zero-wind "critical layer" (see, e.g. Turner, 1973, p.38).

At 1200, the seabreeze cell has enlarged to about 30 km width (Fig. 1(b)). By comparison, the actual width at this time was about 16 km (Fig. 2). This factor of two differences also is apparent at 1300 (assuming a constant rate of seaward progression of the actual sea breeze). The larger growth rate of the model sea breeze rates as one problem for further study; the observed inland progress of the model front can be seen to decrease with time, being about 10 km hr^{-1} between 1100 and 1200 and only 2 to 3 km hr^{-1} between 1300 and 1400. This suggests that the error may be a result of the large grid side which limits the accuracy with which the early development is resolved.

By 1300 the vertical motions have developed to produce an intense rotor directly above the sea breeze cell, and the sea breeze has intersified. Intensification of the easterly under the rotor has split the sea breeze circulation, and relatively intense vertical motions have been generated. The maximum downdraught in the lee of the "head" of the sea breeze is about 0.1 ms^{-1}, and is probably limited by the resolution of the model.

The 1400 result (Fig. 1(d)) showed the sea breeze growing seaward, deepening and intensifying to a maximum wind speed of about 3.5 ms^{-1} (averaged in the 0-350 m layer). However, the rotors were clearly weakening, and their energy appeared to be propagating outward from the computation grid.

4. DISCUSSION

In spite of reservations about the present quantitative accuracy of the model, the results do suggest a mechanism for the observed character of the sea breeze.

At 1100, both rotors were positioned above the sea breeze cell, with a separation of 25 km. The separation was again 35 km at 1200, increasing to about 42 km (average between each pair of cells) at 1300, and about 45-50 km at 1400. During this time, the sea breeze cell grew from about 12 km to 80 km width.

Modelling the shape of the sea breeze cell as a half-sinusoidal form (e.g. sin x for $0 < x < \pi$) has shown that the principal flow perturbation in the easterly above have wavelengths greater than the cell length. This suggests that the decaying stage of the rotors (1400 hours) corresponds to cell length of about twice the resonant wavelength (80 km 2 x 45 to 50 km).

The cause for the sharply "resonant" maximum at 1300 hours is less clear. Inspection of Fig 1(c) shows that an interaction between the rotor and the growing cell has distorted the cell cross-section. This would have increased the amplitude of the resonant component of the perturbation to the easterly flow. The close correspondence of the distance between the "head" and "tail" regions of the front to the roughly 40 km "resonant" wavelength supports this view.

The result of this intense downward motion, followed by redevelopment of the sea breeze after the "resonance", could have produced dynamic entrainment of warm air into the cell. This possibility was tested using an approximate trajectomy, derived from the four circulations shown in Fig. 1. The result shown in Fig. 3, indicates that the air involved in the intense downward easterly at 1300 may indeed have undergone entrainment.

5. SUBSEQUENT INVESTIGATIONS

Arising partly from discussions at the KAMS workshop, and partly from some of the limitations of the above result, a farther study was carried out using a 3 km grid resolution, with a 3 km wide island centred 7.5 km offshore. The result, it was hoped, would clarify the possible effect of Garden Island on the sea breeze as well as demonstrating whether some of the previously mentioned inadequacies were due to the large grid size.

The effect of the island was found to be slight, mainly producing a slightly seaward recentring of the sea breeze cell. The discussed veering of the easterly to seaward of the cell was observed. However, this occurred when the cell extended west of the island, as well as when it terminated in Cockburn Sound. The causes of the southerly tendency appears to be the reduction of the easterly wind by the offshore pressure gradient; this initiates geostrophic adjustment to a more southerly direction.

The major effect of the improved resolution was to slow the rate of inland advance of the cell. This verified the cause of the excessive speed of advance, in the previous run of the model, to be the 10 km resolution.

The agreement with Scott's data was in fact surprisingly good. When first resolved, at 1100, its width was 9 km (actual at this time, 9 km) at 1200 its width was 21 km (actual, greater than 15 km). Between 1100 and 1240, it moved inland at 4 km hr^{-1} (actual in region unaffected by Point Peron, 3½ to 5½ km hr^{-1}).

Furthermore, since the model sea breeze was first observed again at 1100, it seems that an improvement of vertical resolution may be required to detect the early stages (9 - 10 A.M.)

6. CONCLUSIONS

The cause of the warmth of the March 2nd sea breeze appears to be dynamic entrainment (with possible turbulent contributions). This occurred during a period of interaction between the sea breeze cell and motions produced in the vicinity of the level of zero offshore wind. The inclusion of warm continental air in the sea breeze cell may have easily produced the observed result.

Such entrainment would have produced a less homogeneous sea breeze, giving stronger acoustic sounder echoes. It may also have produced effects of environmental significance, such as an increase in the mixing depth.

The more detailed results of this study are being made available elsewhere (Rye, 1978 b).

Acknowledgement: The author is indebted to Mr. Alan Scott, of the Bureau of Meteorology for his provision of the data on the development of the actual March 2nd sea breeze.

REFERENCES

Rye, P.J, 1978(a) The W.A.I.T. Physics Department Atmospheric Numerical Model, W.A.I.T. Physics Department Internal Report PD 165/1978/AM 8.

Rye, P.J, 1978(b) "The KAMS Field Day: Results from a Numerical Sea Breeze Model, W.A.I.T. Physics Department Internal Report (in preparation)

Turner, J.S, 1973. "Buoyancy Effects in Fluids", Cambridge University Press.

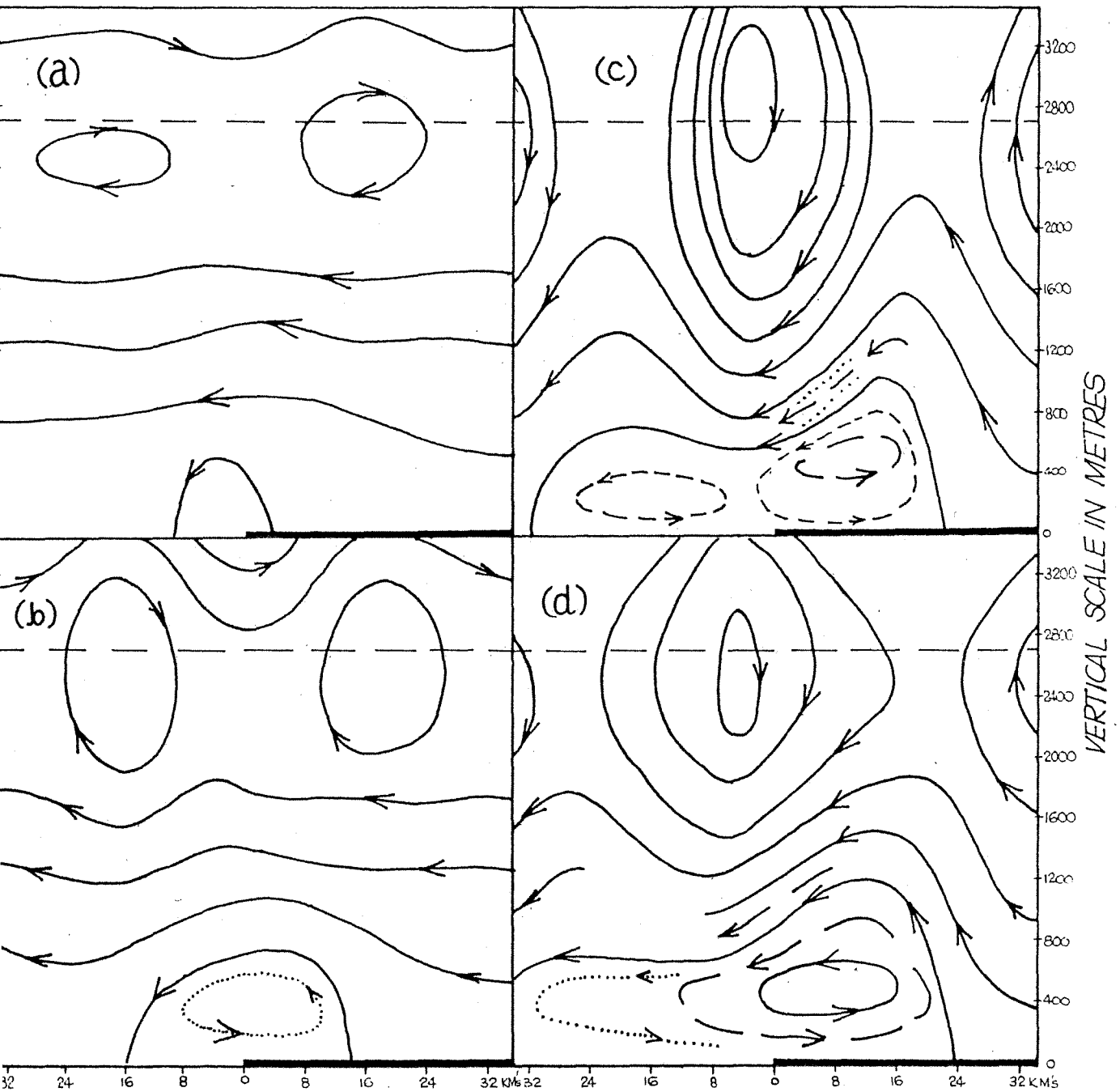

Figure 1: Streamlines for the March 2nd sea breeze, at 1100 W.S.T. (a), 1200 (b), 1300 (c) and 1400 (d), produced by the numerical model. The lines represent contour intervals of the stream function in units of 2 ms^{-1} x (vertical grid interval). Broken lines within the sea breeze cell correspond to an interval of 1 ms^{-1} x (grid interval), while dotted lines represent half this value. The horizontal broken line indicates the original level of zero offshore wind.

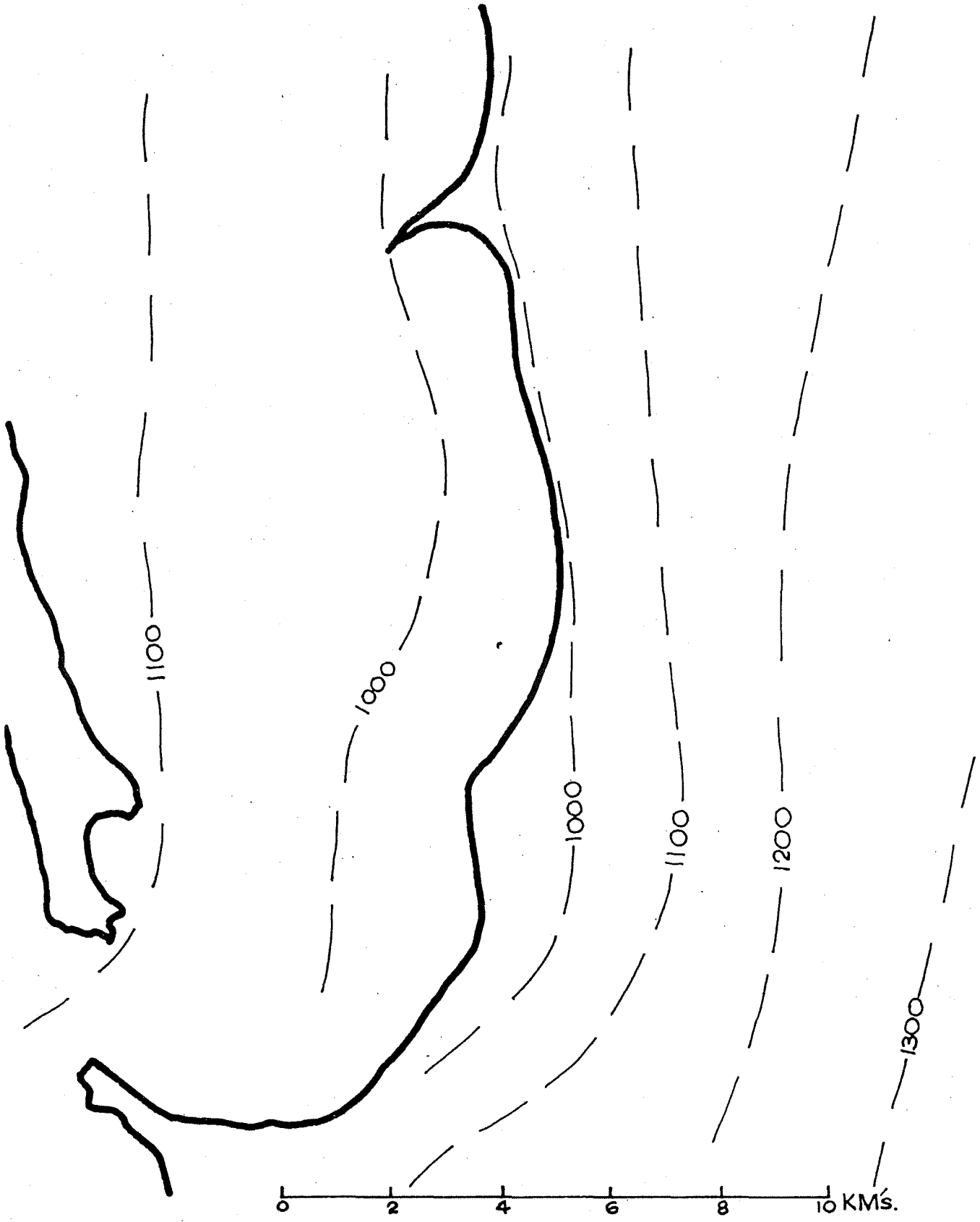

Figure 2: Onshore and offshore development of the actual sea breeze, at 1000, 1100, 1200 and 1300 W.S.T. (supplied by A. Scott).

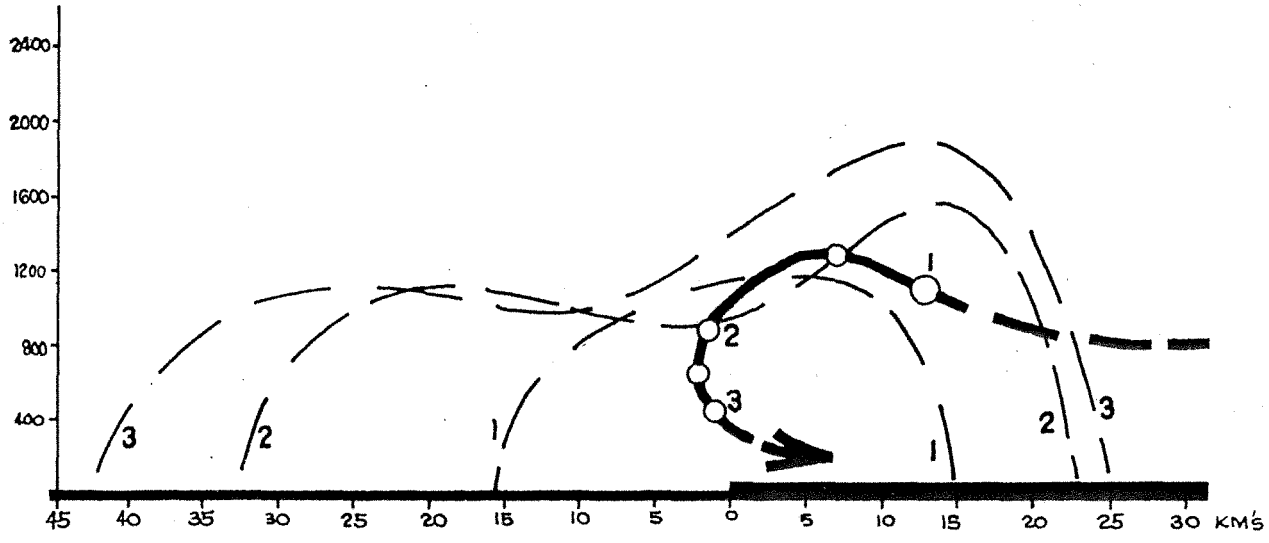

Figure 3: Calculated trajectory for air in the intense easterly above the sea breeze, at 1300. Calculated positions on the trajectory are marked by circles, and the outline of the sea breeze cell is indicated by a broken line. The number 1 refers to 1200 W.S.T., 2 to 1300 and 3 to 1400.

An Interpretation of the WAIT/DCE Acoustic Sounder Record made during the KAMS Intensive Study March 2, 1978

N.E. Holmes, M.J. Lynch, W. Walker

Physics Department, WAIT

1. INTRODUCTION

It is the purpose of this note to provide an interpretation of the WAIT/DCE sounder record made on 2 March, 1978. Use is made of all relevant meteorological data acquired during the study, but even with this supporting information, some of the deductions are speculative.

The record essentially shows the development of a sea breeze and as an interesting aside, it is compared with a similar event recorded at the Wilbinga base station - a record which proves far simpler to interpret.

2. THE RECORD AND ITS INTERPRETATION

The sounder was located approximately 100 m from the beach, at the Kwinana base station on the Fremantle Port Authority site. Recording commenced at about 11.00 hours and continued through out the intensive study period. A copy of the record is presented as figure 1.

From wind speed and direction data recorded at the same time, (presented as figure 2) it is clear that the sea breeze commenced at about 09.30, when the wind direction record shows a rapid shift from a mainly easterly flow to a westerly, which backed southerly as the day progressed. Since the sounder was not operating until about 11.00 hours, the onset of the breeze is not recorded.

The first feature to appear on the record (at about 11.00) is the echoing structure associated with the marine/land air interface. This is observed to rise, in a wavy fashion, from a height of 100 m at 11.00 to about 350 m at 12.15, when the echoes become too weak to be definitely recorded. The air below the interface appears fairly free of echo suggesting that the lapse rate is close to dry adiabatic, although the presence of some weak echoes and the subsequent development of much stronger ones, indicates that the lapse rate may have been weakly stable.

The strength of the inversion/stability produced by the breeze at the marine/land air interface cannot be obtained from the sounder. However radiosonde ascents from the mudlake site (presented as figure 3) show a weak elevated stable layer at between 350 and 500 m; depending on time.

This presumably corresponds with the top of the marine layer. Below this there is a region, several hundred metres thick, which is essentially neutrally stable. This overlies a super adiabatic layer in the lowest hundred or so metres. The WAIT/DCE sounder does not show any evidence for the super adiabatic layer, which is not surprising in view of the close proximity of the ocean. The short (approximately 100 m) overland trajectory, would be insufficient to modify the marine air, at least for a westerly flow. However as the day progresses the flow swings further south, increasing the overland path. This possibly accounts for the convection observed later in the day.

Significant echoing structure appears on the sounder record after about 13.00. This thickens from less than 100 m to about 300 m at 15.43. The transition from an almost echo free layer, to a strongly echoing one is difficult to explain and does not appear to be associated with any particular feature in other meteorological data. Possibly the effect is linked with the steady increase in wind speed during the day, which might give rise to turbulence once the Richardson number falls below 0.25. This would give rise to echoes in the weakly stable marine air. In any case it appears reasonable to interpret the depth of the echo as being the depth of the marine air.

Finally the tracer release, which occurred at 14.15, would have been made into the marine air. Examination of the plume sketches (see figure 4) shows no evidence of a strongly stable layer and it must either be assumed that the stable layer is so weak that the plume penetrates it without difficulty, or alternatively the plume never gets out of the marine air.

The sounder estimate of a marine layer thickness of approximately 250 m, although accurate for the site, is probably too small, for the more inland region. The most sensible interpretation would appear to be, that because of the greater overland flow, the marine layer is deeper in the region where the plume is dispersing. The deceleration of the plume as it rises (see figure 4) suggests that it is travelling up through a shear region, but there is no evidence to suggest that the plume mixes through the marine/land air interface and into the return (easterly) flow.

3. EXAMPLE OF A SEA BREEZE OBSERVED AT AN INLAND SITE (WILBINGA BASE STATION)

The coastal location of the Kwinana base station prevents the establishment of significant convective activity in the boundary layer for westerly winds, at least for periods like that of the intensive study, when the air is warmer than the sea surface. The Wilbinga base station, approximately 80 km north of Perth and 7 or 8 km inland, allows strong convection to develop and it is interesting to note how this is modified by the onset of the sea breeze. Figure 5 is a sounder record illustrating the modification. Figure 6 is a record of wind direction. This was made with DCE instrumentation located about 150 m west of

the sounder. The record indicates a sea breeze onset at between 12.30 and 13.00 hours which agrees well with the sounder record. It is interesting to note that convection persists, apparently undiminished even after the establishment of the sea breeze.

4. RECOMMENDATIONS

In order to fully exploit the potential of the acoustic sounder the following recommendations are made.

(i) Sounder records are easier to interpret when there is a significant run of the record showing the development of recognizable phenomena, e.g. it is helpful to have a record of the sea breeze onset and the situation prior to this. Recording should commence some 24 hours prior to the intensive study. This would have been the case for the present work except that a technical problem interrupted the early morning record.

(ii) It would have been useful had record been made at a site somewhat inland from the Kwinana base station. Ideally the sounder should be positioned down wind of the stack to sample the air into which the plume is mixing. It is reasonable to expect fairly strong modification to boundary layer properties in the first few kilometres of the coastal plain and careful selection of the sounder site is important in order to obtain representative information.

(iii) Related to recommendation (ii); it would be helpful to have radiosonde releases from both the WAIT/DCE and the Murdoch sites.

Tethered sondes are unlikely to be successful in the fairly strong winds which are likely to prevail during such studies.

Figure 1

ACOUSTIC SOUNDER RECORD

Kwinana Base Station

2-3-78

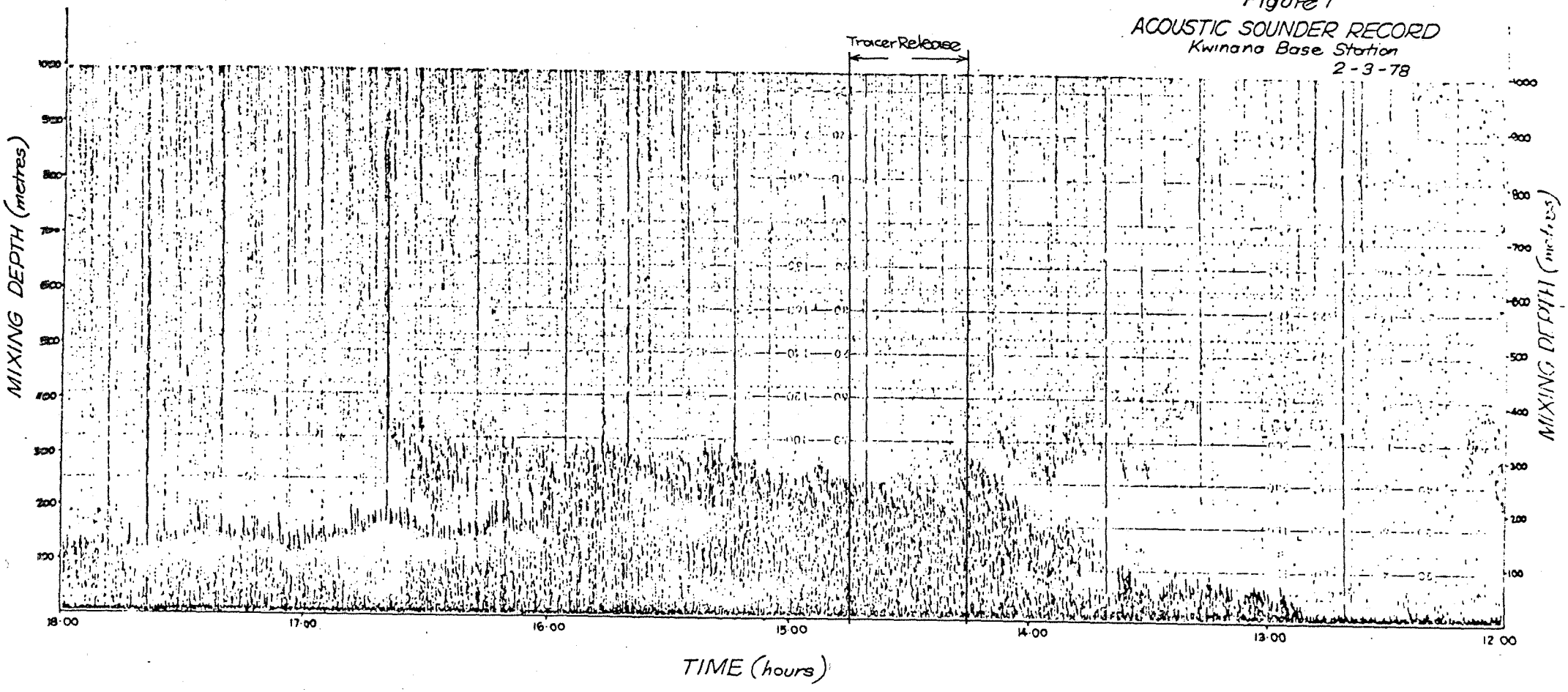

Figure 2

KWINANA BASE STATION

WIND DIRECTION & SPEED

Date : March 2ND 1978.

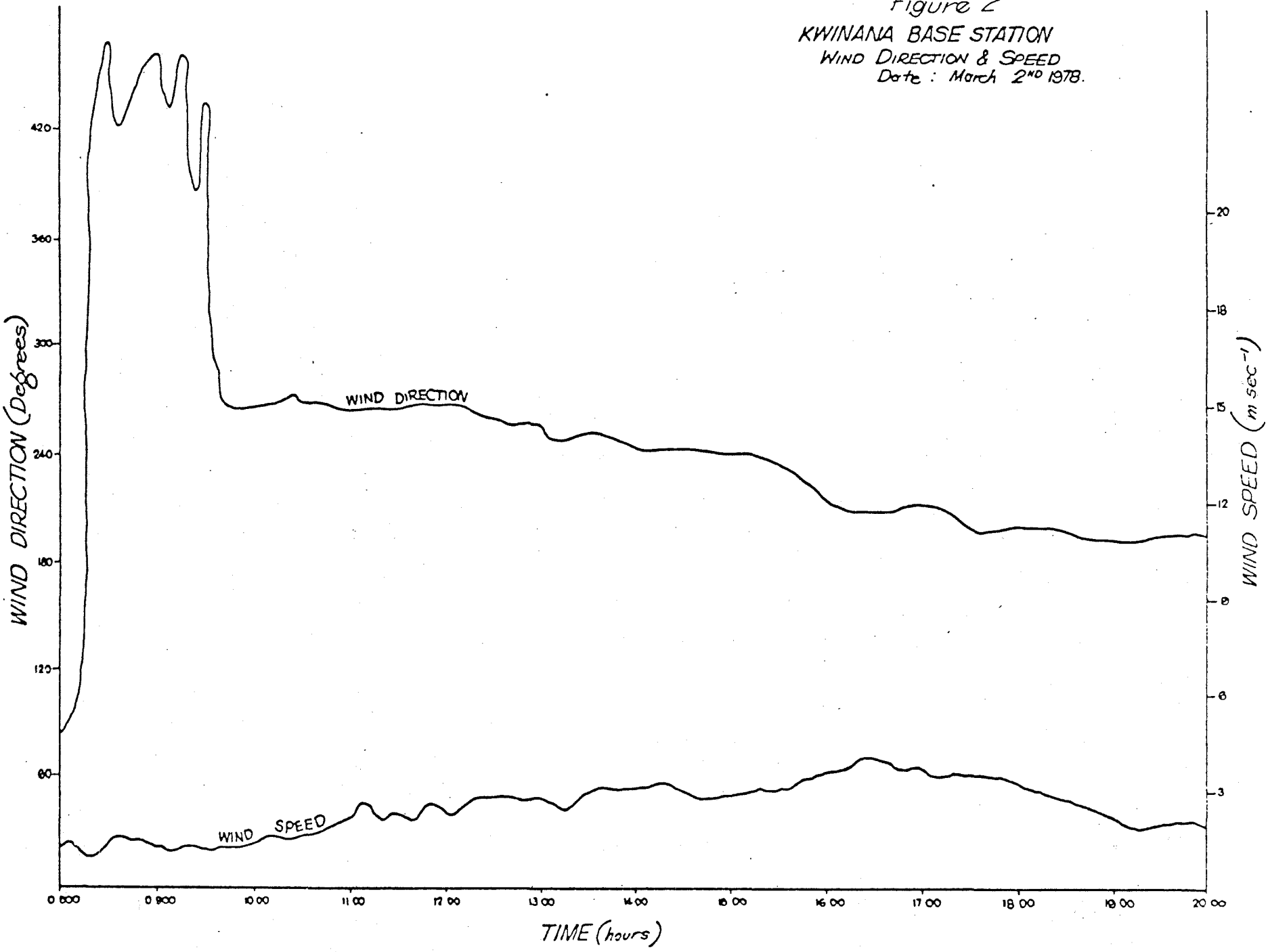

Figure 3

TEMPERATURE vs HEIGHT

Radiosonde data (at times 13·35, 14·18, 14·50)

Alcoa Mudlake "F"

March 2ND 1978.

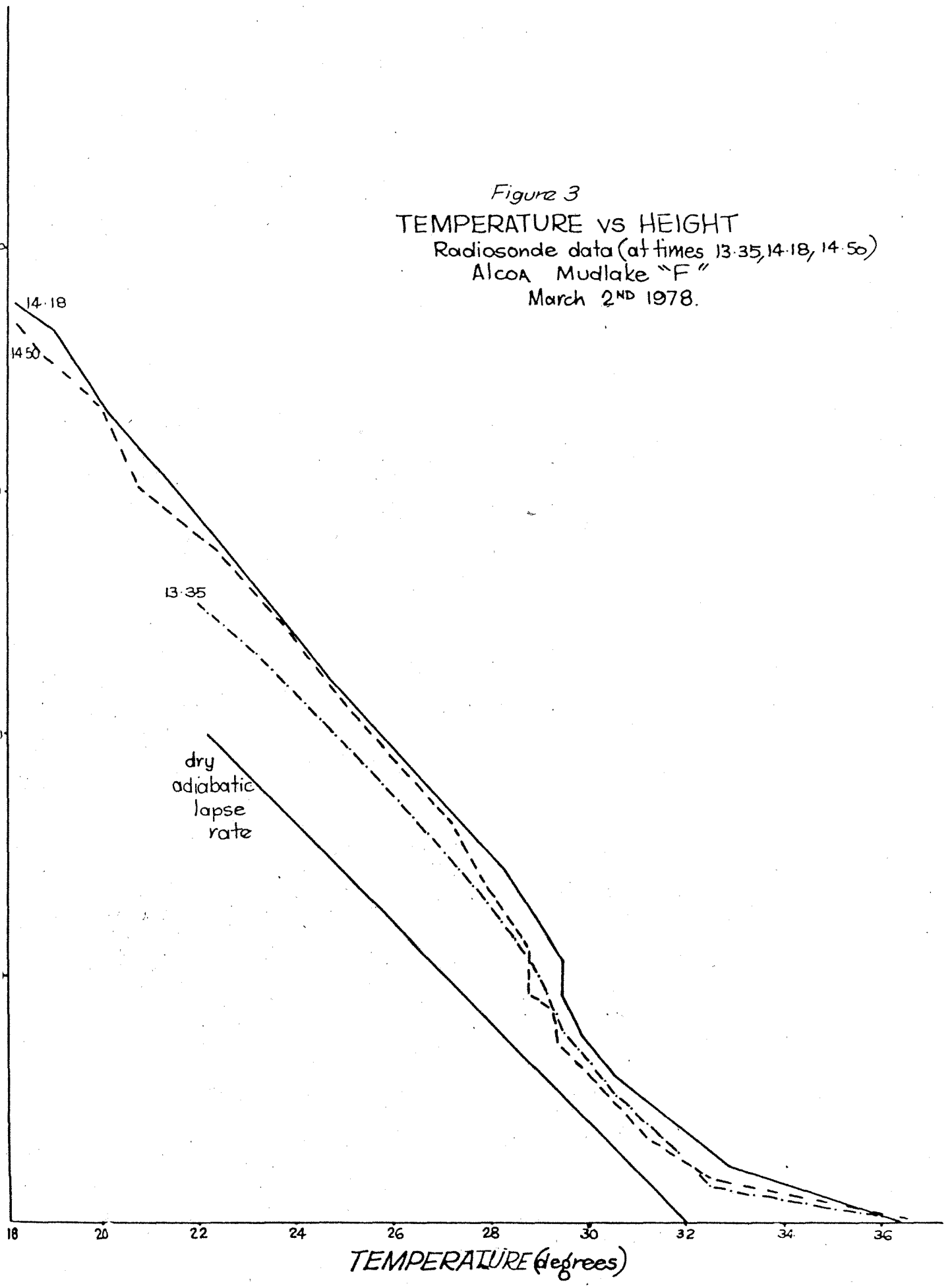

Figure 4

Ground level photography of plume profiles.
Black smoke released from SEC stack (1 km.)
March 2ND 1978
Photography times are shown

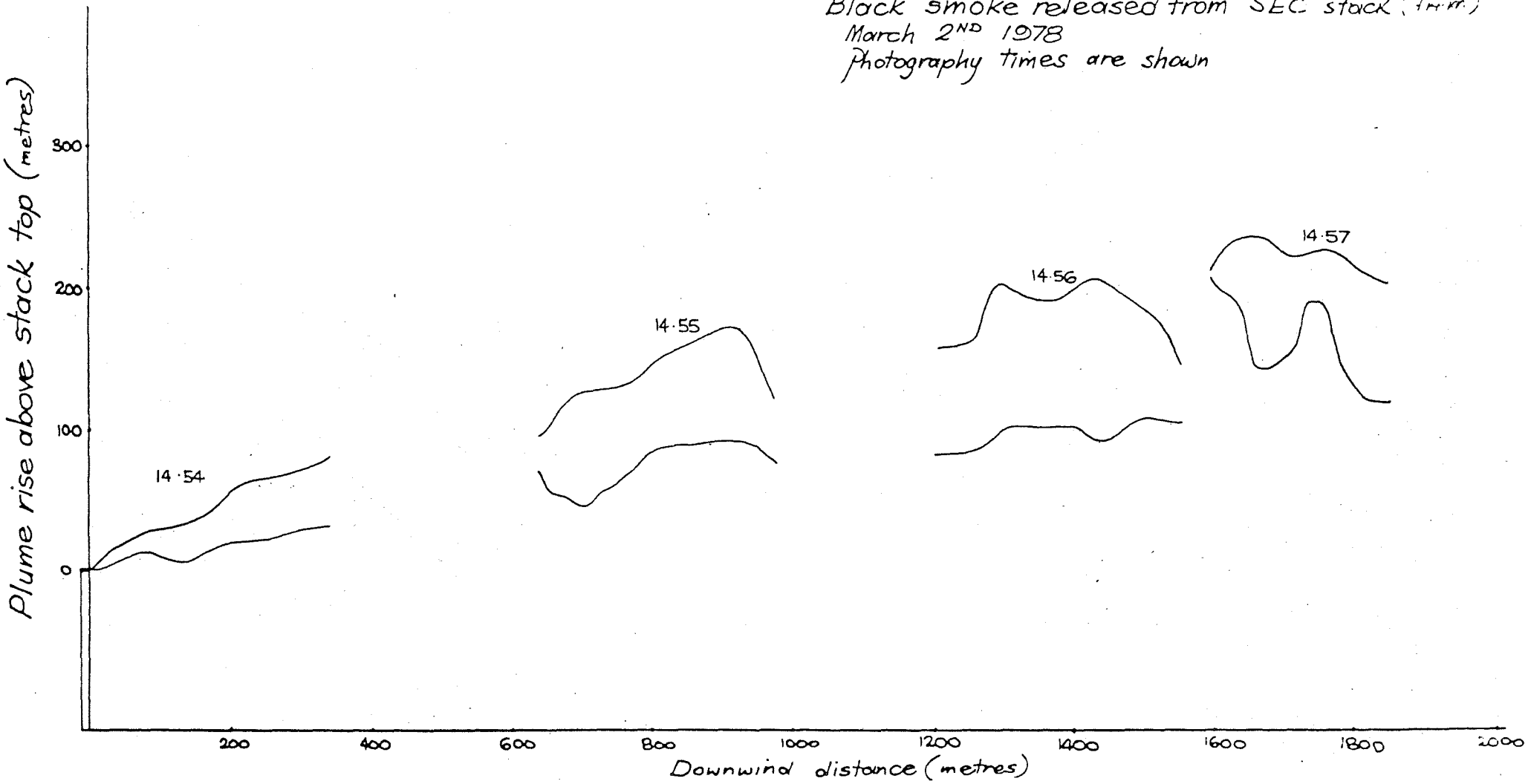

Figure 5

WILBINGA ACOUSTIC SOUNDER RECORD

2-11-77

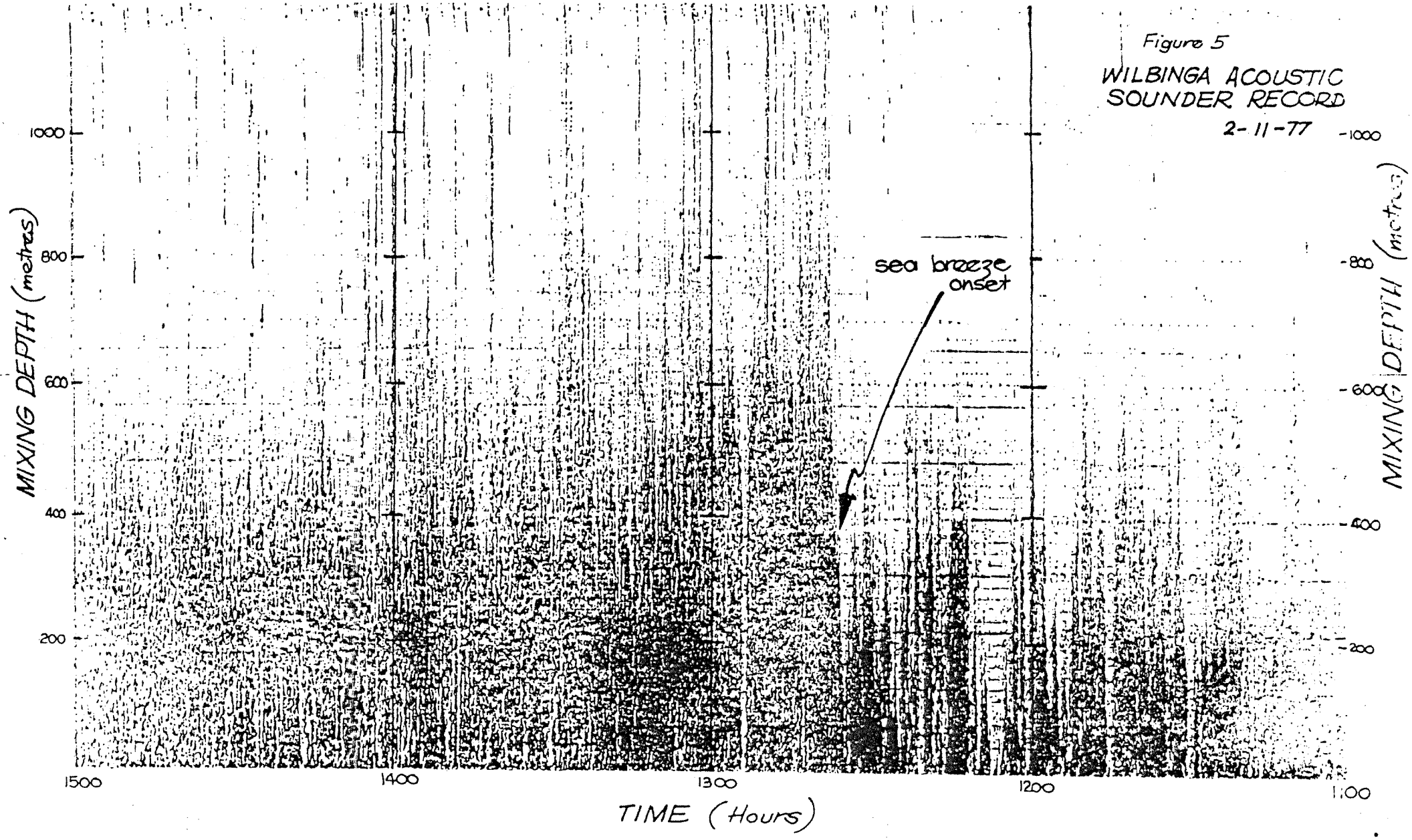

Figure 6

GRAPH OF WIND DIRECTION Vs TIME

For WILBINGA Base station 20-9-77

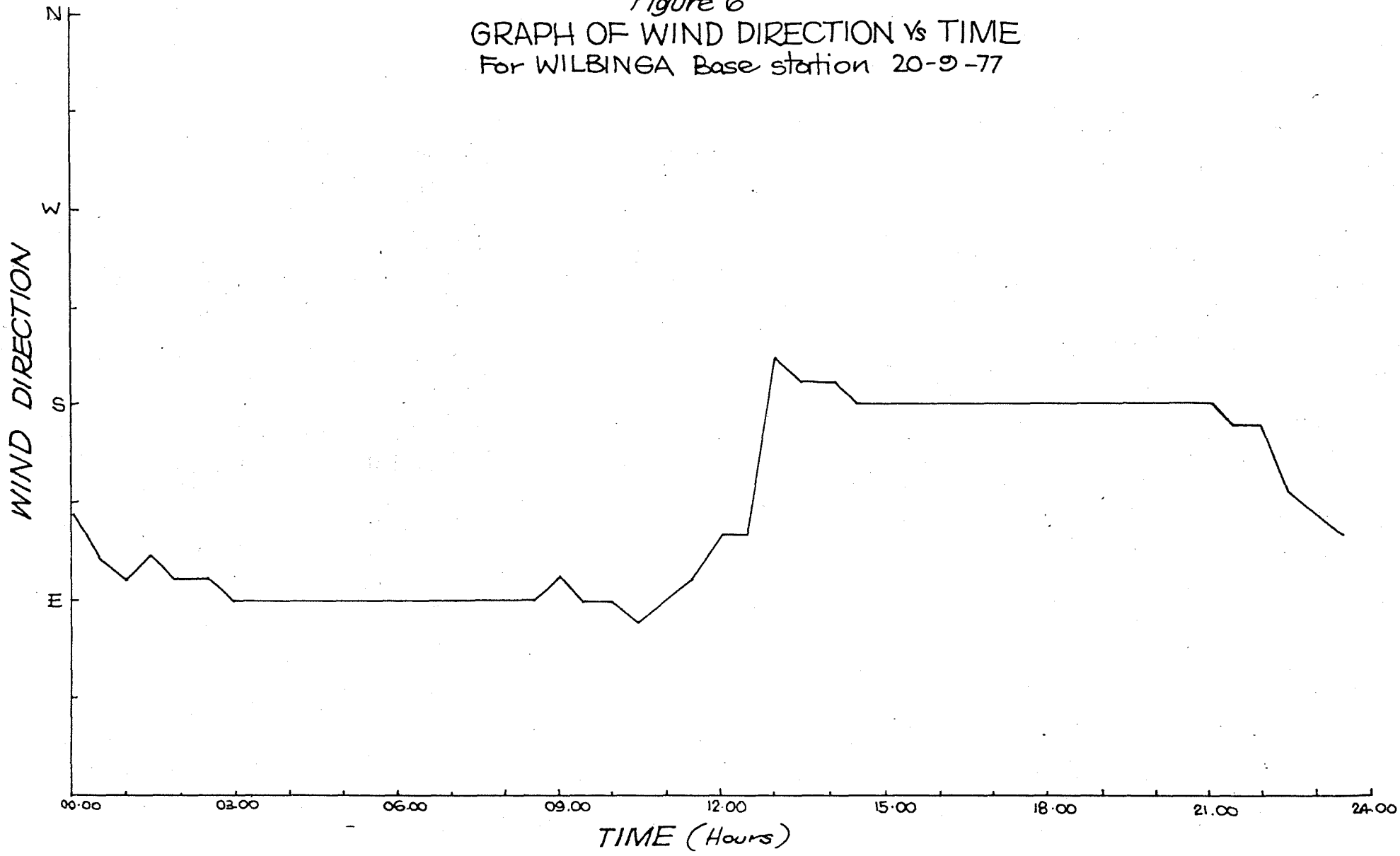

Simulation of Tracer Dispersion

V. Paparo

K. Rayner

Department of Conservation and Environment

1. INTRODUCTION

Two tracers were released from the 114 m SEC stack at Kwinana on March 2, 1978. These were -

(i) SF_6: 31.7 kg over 27 minutes from 2.15 p.m.

(ii) $CFCl_3$: 45.5 kg over 30 minutes from 2.15 p.m.

Air samples at ground level were collected every six minutes at twenty five locations in the Wattleup area during the release of the tracers. Results, given in Environmental Note 33 "Kwinana Air Modelling Study - Tracer Experiment 1", show that SF_6 was recorded at very few sites but that the spread of $CFCl_3$ (Freon 11) was much greater.

In this paper an investigation of a number of plume rise and dispersion models shows the marked impact of atmospheric stability on predicted tracer distribution. The plume rise is strongly affected by the presence of an elevated temperature inversion.

2. PLUME RISE CALCULATIONS

Two methods are used to predict plume rise.

(i) A fluid mechanical approach based on Rayner (1974) enables plume rise to be determined from the simultaneous solution of differential equations expressing the conservation of mass, horizontal and vertical momentum and heat. The major inputs to this numerical model are vertical profiles of temperature, wind speed and wind direction, initial plume density, stack emission rate, diameter and height. Fundamental entrainment and drag coefficients used are those determined by Shalley (1974).

Vertical profiles for temperature, wind speed and wind direction used for these plume rise calculations are shown in Figure 1. These were synthesized using the following available information:

(a) ground level temperature (10m) from the base station 2,

(b) mixing depth (height to the base of the sea breeze/easterly interface) from the WAIT acoustic sounder,

(c) upper atmosphere structure from radiosonde ascent.

Figure 2 shows that the plume rise is restrained by the temperature inversion at 250 m. The variation of wind direction with height produces the lateral veer in the plume centreline shown in Figure 4.

(ii) A method outlined by Briggs (1969) is also used to calculate plume rise. This method was developed for a neutral atmosphere and does not take into account a stable layer at 250 m as assumed in Figure 1(a). Briggs' formulae is:

$$\Delta H = \frac{1.6\ F^{\frac{1}{3}}\ x^{\frac{2}{3}}}{u} \qquad \text{for } x < x_* \qquad (2.1)$$

$$H = \frac{1.6\ F^{\frac{1}{3}}\ x_*^{\frac{2}{3}}}{u} \quad \frac{\left(\frac{2}{5} + \frac{16}{25}\left(\frac{x}{x_*}\right) + \frac{11}{5}\left(\frac{x}{x_*}\right)^2\right)}{\left(1 + \frac{4}{5}\left(\frac{x}{x_*}\right)\right)^2} \qquad \text{for } x > x_* \qquad (2.2)$$

where ΔH = plume rise above exit level (metres)

x = downwind distance (metres)

$x_* = 2.16\ F^{\frac{2}{5}}\ h_s^{\frac{3}{5}}$ (metres)

h_s = stack height (metres)

$F = \left(1 - \frac{\rho_s}{\rho}\right)\ g\ w_o\ r_o^2$

g = 9.8 m sec^{-2}

ρ_s = initial plume density (Kg m^{-3})

w_s = plume exit velocity (m sec^{-1})

r_s = radius of stack top (metres)

u = mean surface wind speed (m sec^{-1})

With ρ_s = 0.8 Kgm^{-3}, ρ = 1.165 Kgm^{-3}, r_s = 2.135m, u = 6 m sec^{-1}, w_s = 13.2 m sec^{-1} and h_s = 114 m, Briggs' plume rise becomes -

$$\Delta H = 1.52\ x^{\frac{2}{3}} \qquad \text{for} \quad x < 298\ m \tag{2.3}$$

$$\Delta H = 67.7\ (1 + 0.00268x)^{-2}\ (0.4 + 0.00214x + 0.0000247x^2)$$

$$\text{for } x > 298m \tag{2.4}$$

The plume rise given by (2.3) and (2.4) is shown in Figure 2 for an idealized atmosphere.
Briggs, however has developed a method for determining whether a plume will penetrate an inversion; If the temperature elevation θ', of the plume over the ambient air temperature T is greater than the increase in ambient potential temperature, then the plume penetrates the inversion. Briggs has given:

$$\theta' = \frac{4\ T\ F}{g\ u\ z^2}$$

where Z is the height above the top of the stack. Application of this formula yields the result that the plume is not buoyant enough to penetrate the assumed temperature inversion at 250 m. At this level $\theta' = 0.205^{\circ}C$ and the rise in ambient potential temperature is $0.7^{\circ}C$.

3. DISPERSION CALCULATIONS

The calculation of tracer concentration is accomplished by applying a Gaussian distribution to the plume centreline determined in Section 2.
The method is essentially that of Turner (1970) with some extra terms accounting for reflection at an inversion base (the tracer is assumed to be trapped under a lid).

Hence the concentration is given by:

$$\chi\ (x, y, z; H) = \frac{Q}{2\pi\sigma_y\sigma_z\ u}\ \exp\ (-\frac{1}{2}\ (\frac{y}{\sigma_y})^2)$$

$$\{\exp\ (-\frac{1}{2}\ (\frac{z - (H + \Delta H)}{\sigma_z})^2) + \exp\ (-\frac{1}{2}\ (\frac{z + (H + \Delta H)}{\sigma_z})^2)$$

$$+ \exp\ (-\frac{1}{2}\ (\frac{z - (2Hmix - (H + \Delta H))}{\sigma_z})^2)$$

$$+ \exp\ (-\frac{1}{2}\ (\frac{z + (2Hmix - (H + \Delta H))}{\sigma_z})^2)\ \} \tag{3.1}$$

where $\chi\ (x, y, z; H)$ = tracer concentrations (μgm^{-3})

H = stack height (metres)

ΔH = plume rise above stack top (metres)

Q = emission rate of tracer ($\mu g\ sec^{-1}$)

U = wind speed ($m\ sec^{-1}$)

Hmix = height of inversion base (metres)

σy = standard deviation in cross-wind direction (metres)

σz = standard deviation in vertical plane (metres)

x = downwind distance (metres)

y = cross wind co-ordinate (metres)

z = height above ground level (metres)

The emission rates for the two tracers are:

$Q = 1.956 \times 10^7\ \mu g\ sec^{-1}$ for SF_6

$Q = 2.527 \times 10^7\ \mu g\ sec^{-1}$ for Freon 11 ($CFCl_3$)

The mean wind speed, u, is taken as 6 $m\ sec^{-1}$ for the dispersion calculations.

4. PREDICTED TRACER CONCENTRATIONS

Figure 3 shows centreline ground-level concentration of Freon 11 obtained by equation 3.1 with plume rise given by either the method of Rayner or Briggs. Briggs formula produces a lower maximum concentration at ground level under the same conditions due to the fact that the plume is not constrained by the inversions at 250 m (see Figure 2).

The mixing depth has a marked effect on maximum ground-level concentration, this falling from 18 μgm^{-3} for Hmix = 250 m to 13 μgm^{-3} for Hmix = 300 m. Though the inversion base is assumed to be at 250 m, a mixing depth of 300 m for the dispersion calculations only (equation 3.1) could be a more realistic figure. This would mean that the tracer is assumed to be trapped in a layer of air 300 m thick; that is there is some penetation of the inversion layer.

Concentration contours of Freon 11 based on equation 3.1 and the plume rise of Rayner are displayed in Figure 4. These can be compared to the actual measured values given in Figure 5.

5. SULPHUR DIOXIDE CONCENTRATIONS

Based on the emissions data from two SEC stacks and seven stacks from Alcoa (Appendix 1) ground-level centreline concentrations of SO_2 have been calculated using 3.1 and Briggs plume rise and are shown in Figure 6. A predicted maximum of 850 μgm^{-3} occurs at about 3 km down-

wind of the SEC's 114 m stack. The average value measured at the Wattleup base station from 2.30 to 3.30 on March 2, 1978 was 1024 μgm^{-3} (38.4 pphm). Application of Rayners plume rise to take into account the temperature inversion at 250 m would increase the predicted maximum concentration.

6. REFERENCES

Briggs G.A., (1969) Plume Rise

Rayner, K.N. (1974) Turbulent Buoyant Jet Theory with Application to the Analysis of Smoke Plume Behaviour

Shalley, D. (1974) Private Communication

Turner, D.B. (1970) Workshop on Atmospheric Dispersion Estimates

VERTICAL PROFILES OF TEMPERATURE, WINDSPEED & DIRECTION
USED FOR PLUME CALCULATIONS.

March 2. Tracer Release
Figure 1

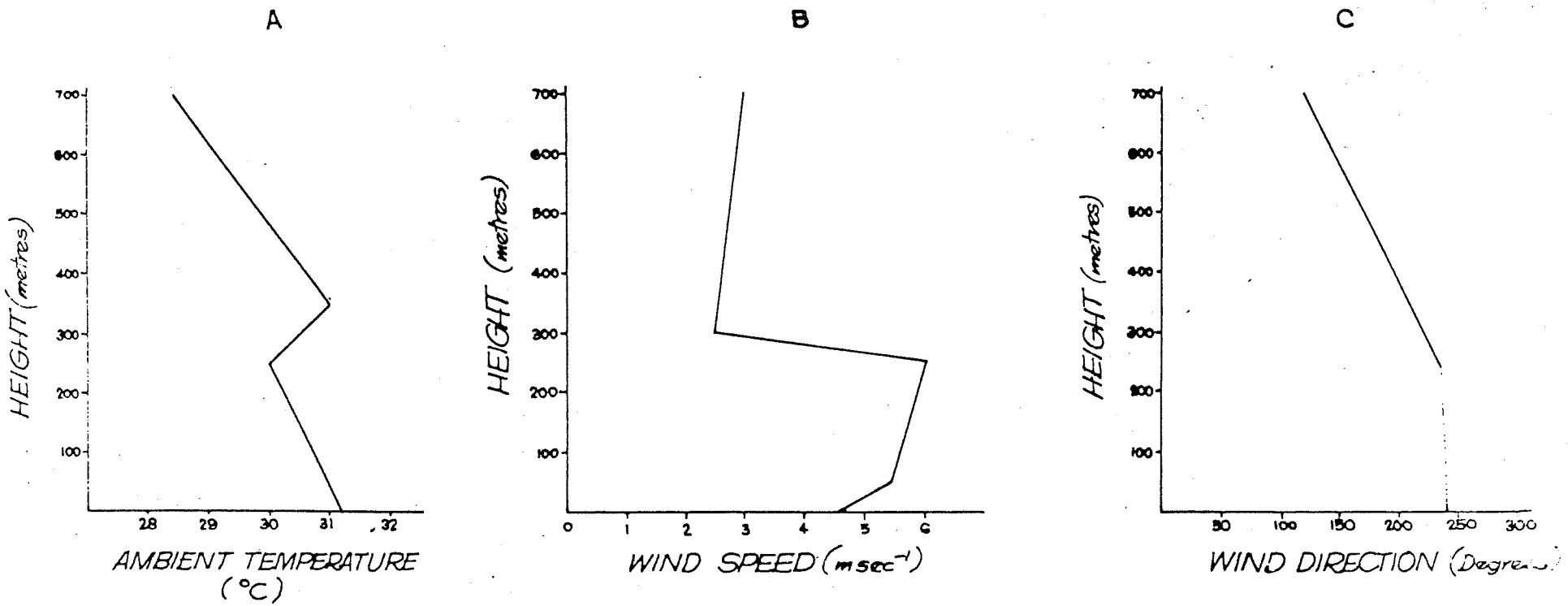

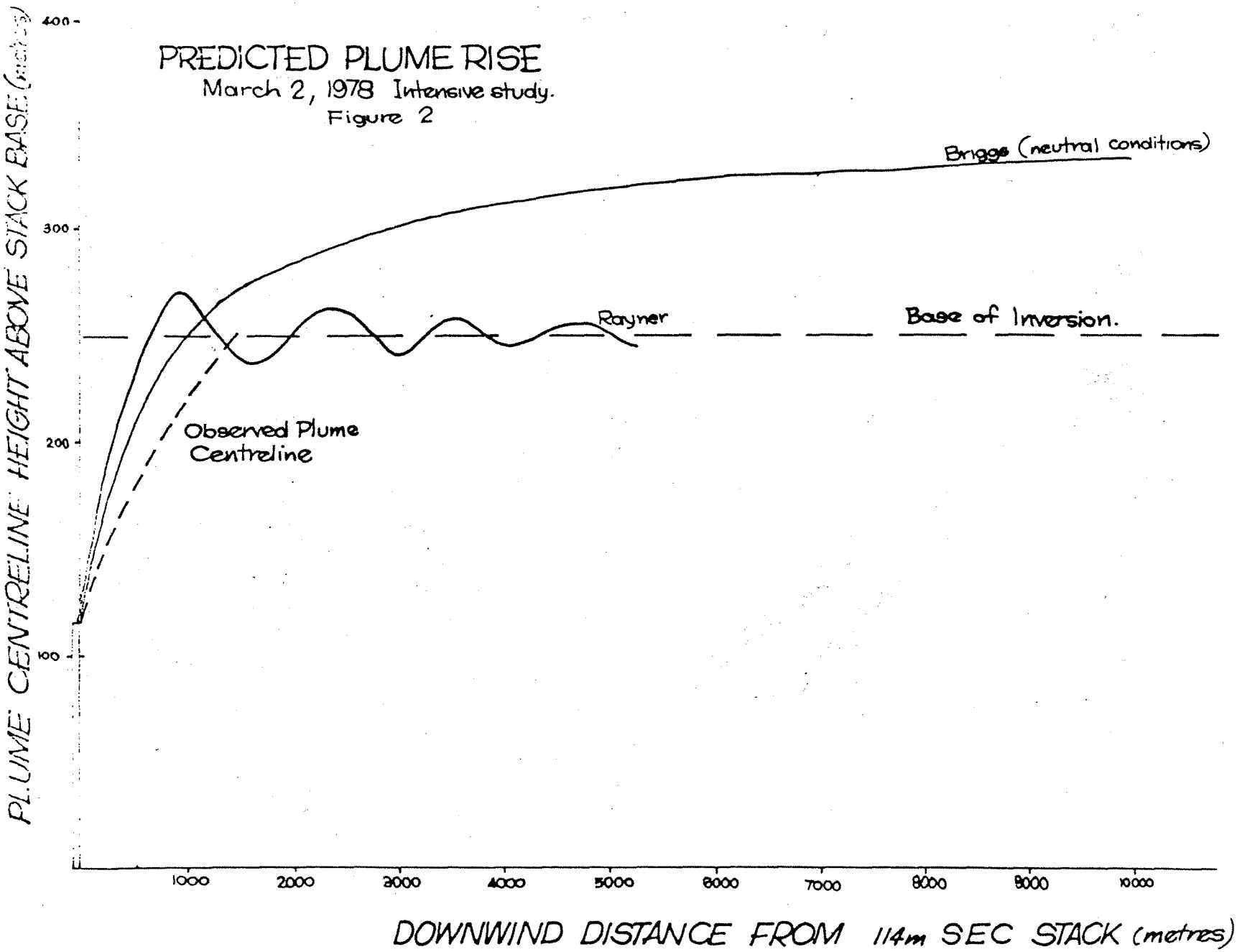
PREDICTED PLUME RISE
March 2, 1978 Intensive study.
Figure 2
PLUME CENTRELINE HEIGHT ABOVE STACK BASE (metres)
400
300
200
100
Briggs (neutral conditions)
Rayner
Base of Inversion.
Observed Plume
Centreline
1000
2000
3000
4000
5000
6000
7000
8000
9000
10000
DOWNWIND DISTANCE FROM 114m SEC STACK (metres)

PREDICTED CENTRELINE GROUND LEVEL CONCENTRATION OF FREON 11

March 2, 1978 Tracer Release

Figure 3

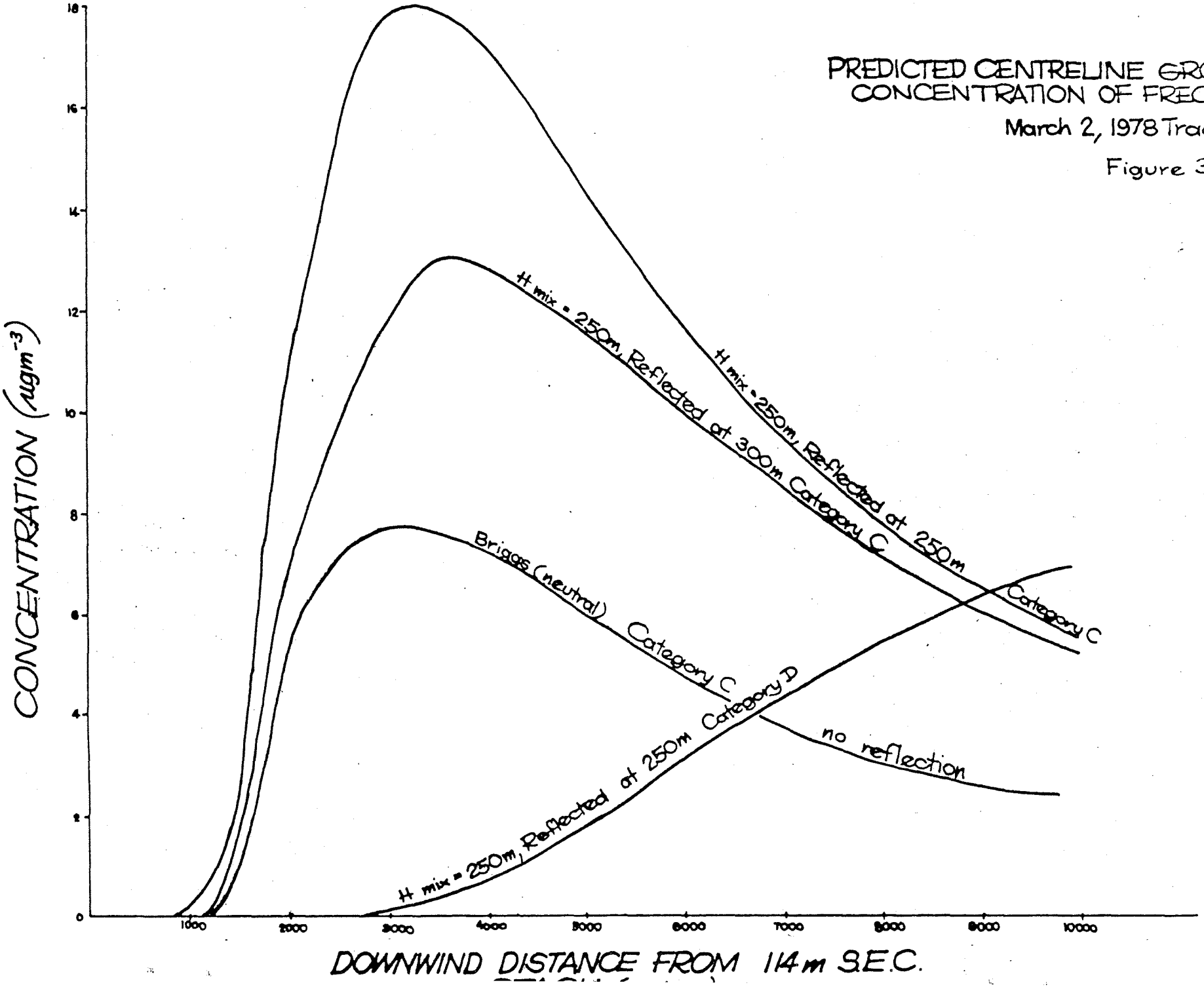

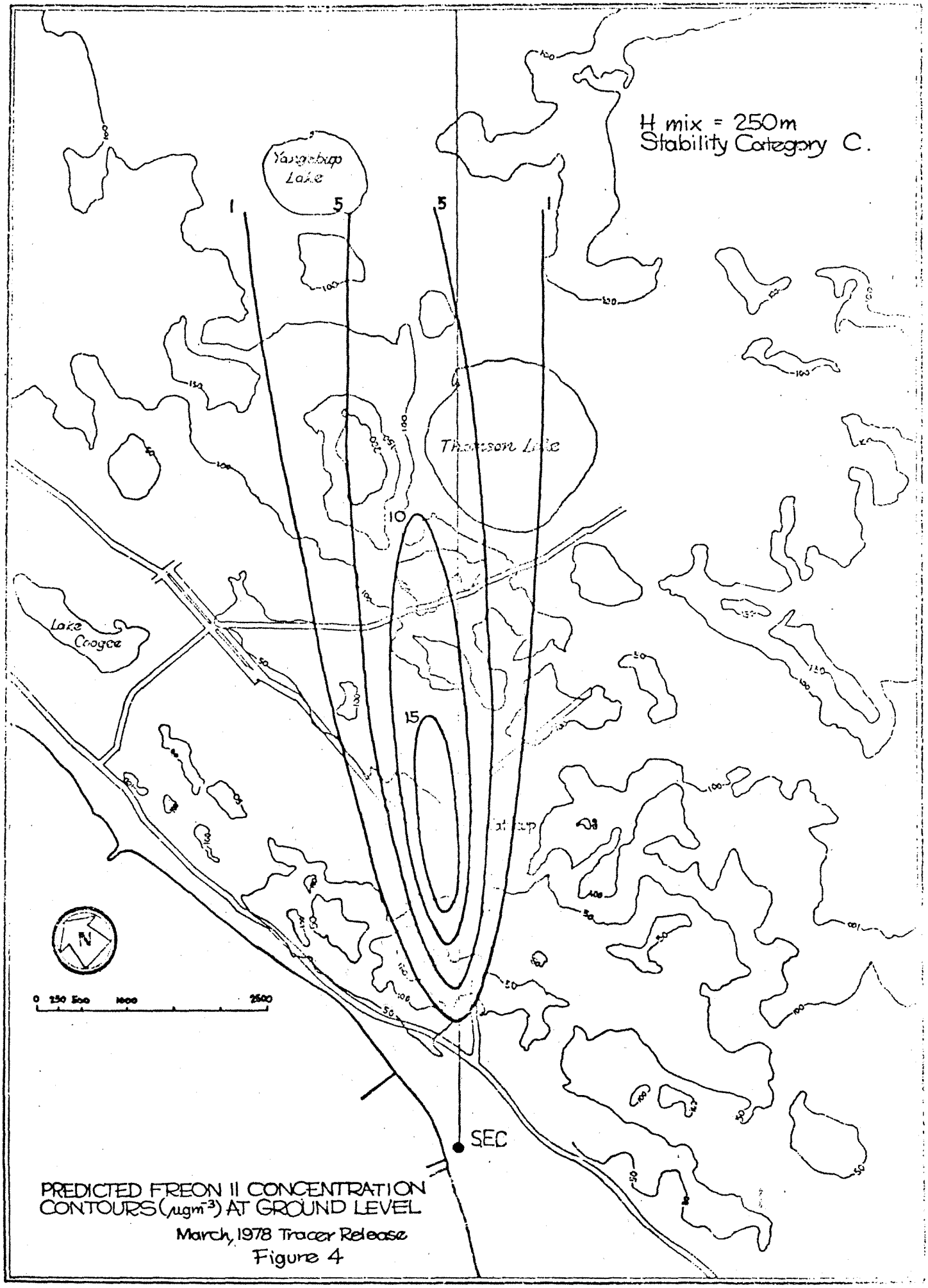

PREDICTED FREON 11 CONCENTRATION CONTOURS (μgm^{-3}) AT GROUND LEVEL

March, 1978 Tracer Release

Figure 4

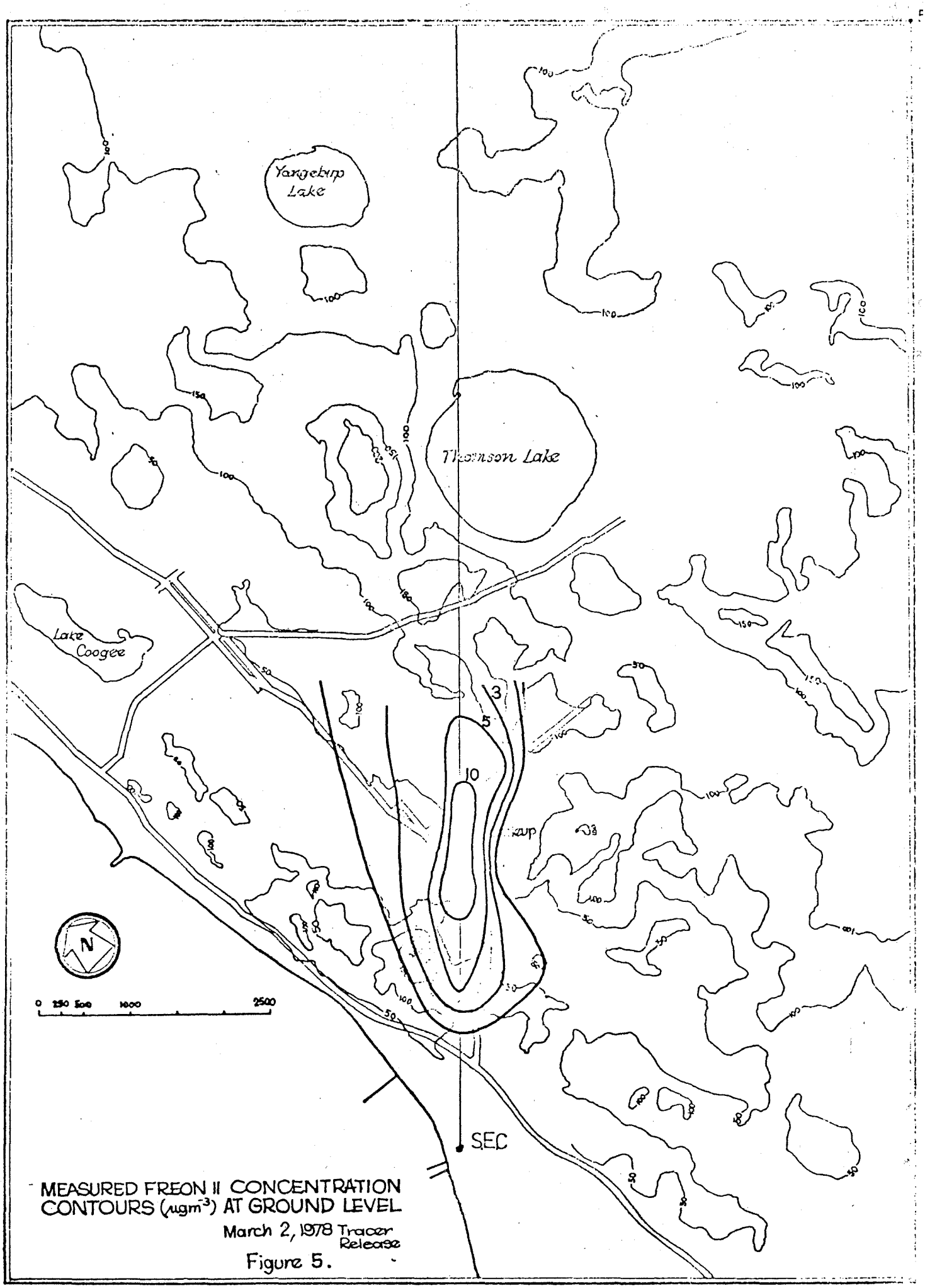

MEASURED FREON 11 CONCENTRATION CONTOURS (μgm^{-3}) AT GROUND LEVEL

March 2, 1978 Tracer Release

Figure 5.

PREDICTED SO_2 GROUND LEVEL CONCENTRATIONS (μgm^{-3})
Based on Model for
March 2 Intensive study.

Figure 6

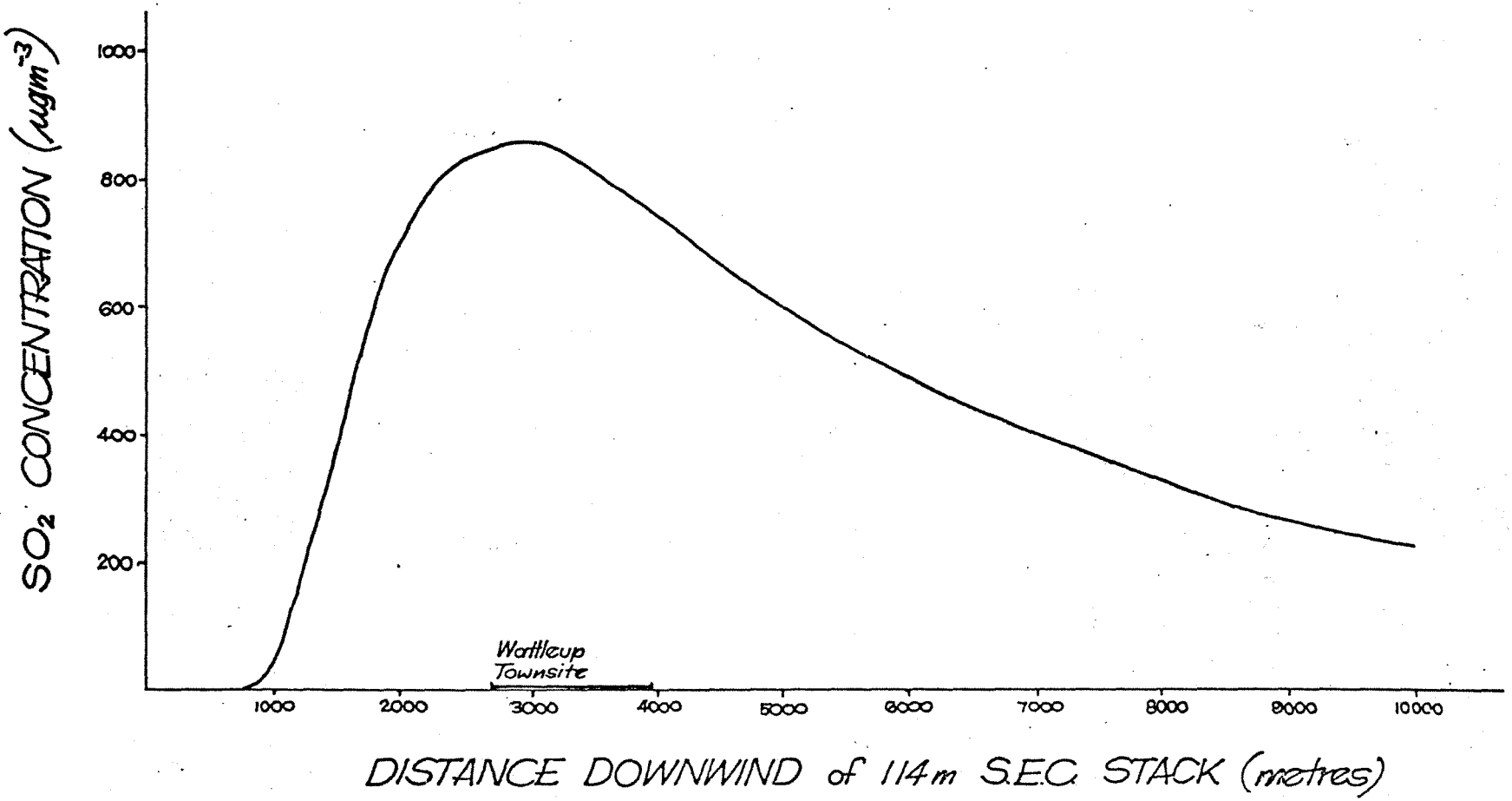

Comment on the Data Collected During the March 2, 1978 Intensive Study

Greg Allen

Physics Department, WAIT

1. SUMMARY

The compilation of the March 2 1978 data has been examined from the point of view of (i) consistency of the data, and (ii) usefulness in parameterising the Kwinana area dispersal of pollutants.

The correlation of the two tracer gases at each location and sampling time shows that the ratio of the reported concentrations is nearly constant and not much different from calculated values using emission rates. If anything there is probably a greater ratio of Freon 11 to SF_6 than expected.

Comparison of the SF_6 emission rate and observed concentration with SO_2 values from the SEC units 1-4 indicated that the Wattleup SO_2 ground level concentrations are probably not all due to the SEC emission.

2. THE TRACER RELEASE

The emission rates of sulphur hexafluoride (SF_6) and Freon 11 at the 114 m SEC stack indicate that the ratio of observed concentration of Freon 11 to SF_6 should be 1.29, assuming constant well mixed tracer release over the period. This is compared with the observed ratios in a plot of Freon 11 concentration as a function of SF_6 concentrations in Figure 1. There appears to be an instrument uncertainty of 0.17 g/m^3 for SF_6 and between 0.5 to 1.2 g/m^3 for Freon 11, but these values are not large enough to account for the discrepancy between observation and experiment. The least squares fit to the data (using only values larger than instrument reading error and deleting the point with extraordinarily high SF_6 at site 22) gives

$$\left[CFCl_3 \right] = 1.92 + 1.36 \left[SF_6 \right]$$

with correlation coefficient 0.85 over 12 points, and this is significant at the 1% level.

The discrepancies between predicted ratios of the concentrations and the observed values would be caused by many factors, some of which could be investigated. These error sources include: unmixed tracer gas before release into the flue gases; unequal release rates of the tracer gases due to flow control; total release volume uncertainty: loss of tracer gas in the bag samplers; error in the zero and span gas in the gas chromatograph; chromatograph nonlinearity; and contamination of the tracer from other sources.

The dilution factor derived from the tracer samples at site 14 for SF_6 is defined to be the ratio of SF_6 emission rate to measure four minute average SF_6. This is calculated to be 6.6 (kg/hr)/(ug/m^3). Applying this factor to the total emission rate of SO_2 from SEC units 1-4, using 3.8 tonne/hour gives predicted ground level SO_2 concentration at site 14 as 576 ug/m^3. The 10 minute average ground level SO_2 at the Wattleup base station at this time was 20 to 75 pphm, i.e. 563 to 2110 ug/m^3 (1 ug SO_2/m^3 = 0.0355 pphm).

From this we must conclude that either the tracer was not well mixed with the flue gases, or that the emission from the SEC stacks is not responsible for all of the SO_2 observed at Wattleup. This latter prospect is the more likely when the amount and nature of SO_2 emissions from the Alcoa calciners and powerhouse are taken into account. The Alcoa stacks and the SEC stacks were almost directly upwind of site 14 at the time of maximum SO_2 and SF_6 observations.

3. BASE STATION RECORDS

The reporting of 10 minute average SO_2 together with wind speed and direction, and wind variance (sigma) allows comparison of these observations with tracer release data.

It is worth noting that high sigma and wind from an SO_2 source correlate with high SO_2 observed values.

The ten minute average data is not useful for epidemiological studies since it is usually assumed that long term concentrations of 10 pphm or 1 hour average at 100 pphm will cause damage to sensitive plants while for mortality in humans SO_2 usually needs to be considered together with smoke concentration.

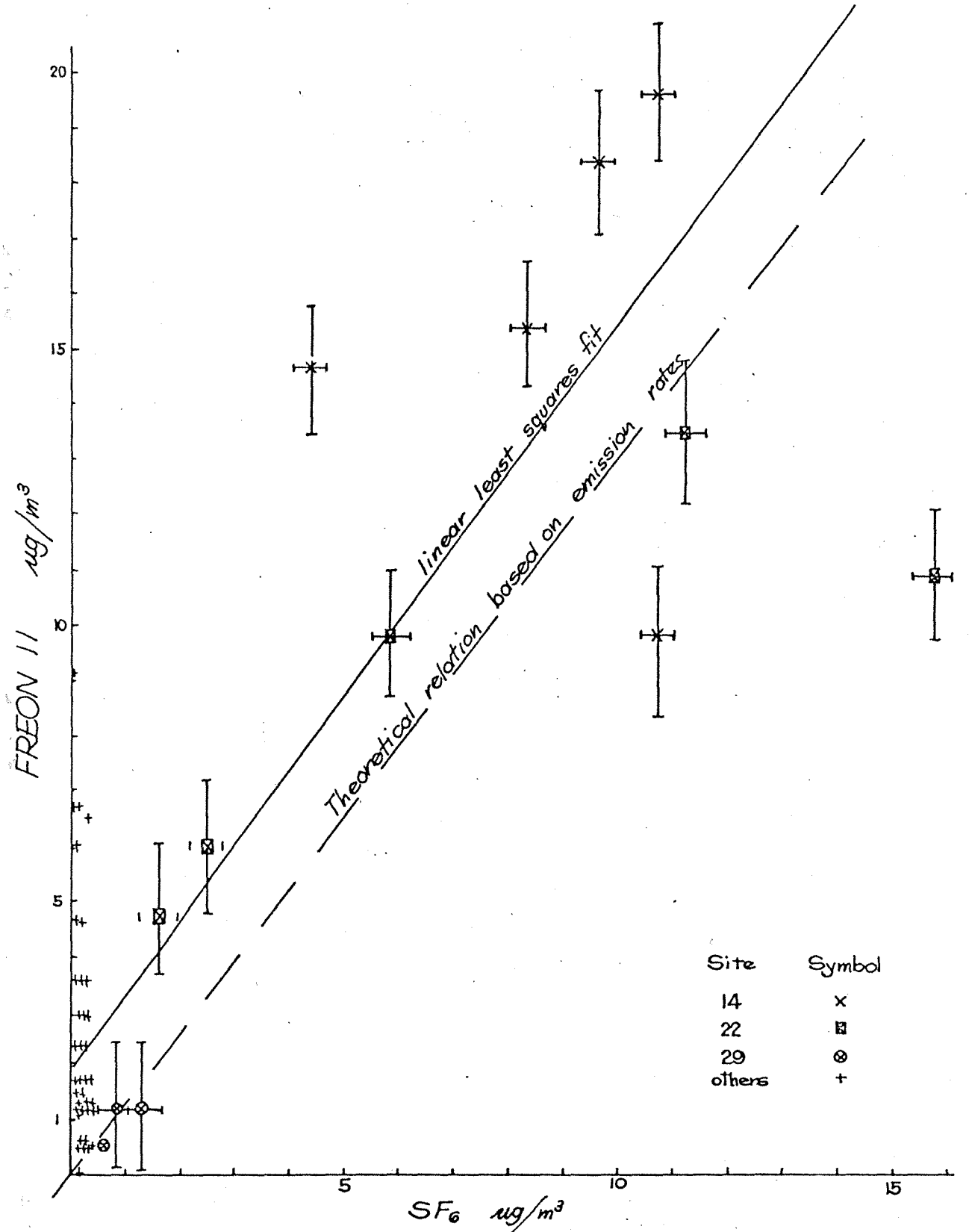

Figure 1. Comparison of observed SF_6 and $CFCl_3$ concentrations.